UPPER CAMPANIAN(?)-LOWER DANIAN PLANKTONIC FORAMINIFERAL BIOSTRATIGRAPHY AND QUANTITATIVE PALEOBATHYMETRY AND PALEOECOLOGY OF THE DABABIYA QUARRY COREHOLE, UPPER NILE VALLEY, EGYPT

by

FIRAT GOCMENOGLU

A thesis submitted to the

Graduate School-New Brunswick

Rutgers, The State University of New Jersey

In partial fulfillment of the requirements

For the degree of Master of Science

Graduate Program in Geological Sciences

Written under the direction of

Prof. Marie-Pierre AUBRY

And approved by

_____

_____

_____

_____

New Brunswick, New Jersey

JANUARY, 2015

ABSTRACT OF THE THESIS

UPPER CAMPANIAN(?)-LOWER DANIAN PLANKTONIC FORAMINIFERAL BIOSTRATIGRAPHY AND QUANTITATIVE PALEOBATHYMETRY AND PALEOECOLOGY OF THE DABABIYA QUARRY COREHOLE, UPPER NILE VALLEY, EGYPT

By

FIRAT GOCMENOGLU

Thesis Director: Prof. Marie-Pierre AUBRY

The 140 m Dababaiya Corehole (DBQ), drilled in the Dababiya Quarry about 35 km south of Luxor, Upper Nile Valley, Egypt, spans the stratigraphic interval from upper Campanian/lower Maastrichtian (the *Globotruncana aegyptiaca* Zone) to the lower Eocene. This study is devoted to an investigation of the planktonic and benthic foraminifera of the Upper Cretaceous (Maastrichtian) and basal Paleocene (lowermost Danian) and complements previously published biostratigraphic studies on the core (Berggren and Ouda, eds., 2012). The investigation is divided into three parts: 1)

new/innovative chemical techniques applicable to the preparation/treatment of indurated claystones and limestones which led to the extraction of generally well preserved foraminifera; 2) planktonic foraminiferal biostratigraphy and temporal continuity of the stratigraphic succession which led to the identification of a probable, brief hiatus(?) within the lower part of basal Danian Zone P0; 3) quantitative paleobathymetric of benthic and planktonic (P/B ratios) foraminifera suggesting outer neritic to upper bathyal Maastrichtian depositional depths consistent with previous estimates for the Paleocene.

ACKNOWLEDGEMENTS

I would like to express my gratitude to principal thesis advisor **Prof. Marie-Pierre AUBRY** for her guidance, encouragements and endless support in every stage of this thesis. She is always going to be staying in my mind with her endless eagerness to research and with her motivating, and kind behaviours towards the people she works with. It is a great honor to feel her trust, support and appreciation.

I would also like to express my sincere gratitude to my co-advisors **Prof. Richard K. OLSSON and Prof. William B. BERGGREN** for their valuable recommendations, comments and contriubitons.

I would like to thank my thesis committee member **Prof. Kenneth G. Miller** for his endless patience and understanding.

I am deeply grateful and thankful to **Turkish Petroleum Corporation (TPAO)** for having given me the opportunity of studying abroad, and having provided the great chance of working with the *World Class* scientists.

I also owe to thank **faculties and staff of Department of Earth and Planetary Sciences** for their nice and kind attitudes, and helps whenever I needed.

I cannot finish writing these words without conveying my gratefulness to my lab-mate and a colleague **Mr. Weimin SI** for helping me to increase my levels of patience as well as opening me the gates of deep understanding of science, and developing different critical views.

Recent and former members of micropaleontology and biostratigraphy research group **Dr. David BORD**, **Mrs. Sarah KLINGLER**, **Mrs. Julie CRISCIONE**, and **Rehab SALEM** are among the people, who are deserving my deep appreciation for their warmness and friendship in the last two-and-a-half year.

My dearest friends **Mr. Canalp ÖZKUL**, **Mrs. Pınar Deniz TOSUN**, **Mr. Ozan ERAT**, and **Mr. Emrah TAŞDEMİR** are also deserving my thankfulness due to making me always feel the warmness of their friendships although we have not been seeing us each other maybe more than a year.

I would like to convey my greetings to the biostratigraphy team members of **STATOIL** (Stavanger, Norway), especially to **Mr. Erik ANTHONISSEN**, for sharing his and their knowledges as well as for their kind attitude to me.

And lastly, my deepest and most sincere gratefullness and appreciation goes to my parents **Mr. Mehmet GÖÇMENOĞLU** and **Mrs. Fatma GÖÇMENOĞLU** for always being next to me although I was continents and oceans away from them. Unfortunately,

neither any pages nor any words I know in any languages could suffice to express my thankfullness to my parents.

TABLE OF CONTENTS

LIST OF FIGURES

Li and Keller (1998a,b) subdivided the Maastrichtian stage into two stages (lower and upper) and nine biozones (CF zones). These are CF9 *Globigerinelloides subcarinata*, CF8 *Globotruncana aegyptiaca*, CF7 *Gansserina gansseri*, CF6 *Rosita contusa*, CF5 *Pseudotextularia intermedia*, CF4 *Racemiguembelina fructicosa*, CF3 *Pseudoguembelina hariaensis*, CF2 *Pseudoguembelina palpebra* and CF1 *Plummerita hantkeninoides*, respectively.

Arenillas et al. (2004) also subdivided *Abathomphalus mayaroensis* and the upper part of the *Gansserina gansseri* biozones. In stratigraphically ascending order *Rugoglobigerina scotti*, *Planoglobulina acervulioides*, *Racemiguembelina fructicosa*, are consisting the upper part of the *Gansserina gansseri* zone and *Abathomphalus mayaroensis*, *Pseudoguembelina hariaensis* and *Plummerita hantkeninoides* are the subzones of *Abathomphalus mayaroensis* zone.

Arenillas et al. (2004) subdivided the P0 *Guembelitria cretacea* zone into *Hedbergella holmdelensis* (lower) and *Parvularugoglobigerina longiapertura* (upper); Pα *Parvularugoglobigerina eugubina* zone into *Parvularugoglobigerina sabina* (lower) and *Eoglobigerina simplicissima* (upper). However, Wade et al. (2011) did not apply such a practice in their studies.

LIST OF TABLES

LIST OF APPENDICES AND PLATES

CHAPTER 1

A New Methodology for Extracting Foraminifera From Lithified Carbonate Rocks and Fine-Grained Sediments: Consecutive Uses of Dilute Acid and Basic Solutions (DAB)

Fırat GOCMENOGLU[1,2]

1) *Department of Earth & Planetary Sciences,*
Rutgers, The State University of New Jersey
Wright-Rieman Laboratories, 610 Taylor Road., Piscataway, NJ 08854-8066

2) *Türkiye Petrolleri Genel Müdürlüğü* (TPAO)*, Araştırma Daire Başkanlığı*
Söğütözü Mahallesi, 2180. Cadde, No.10
06100 Çankaya-Ankara/TÜRKİYE.

Abstract
Morphologic characters are of primary importance in identifying foraminifera. Within the last few decades, the use of either dilute acidic (acetolysis) or basic solutions has become widespread for extracting microfossils exhibiting less than optimum preservation in strongly lithified rocks, particularly limestones and claystones. Previous studies have involved the use of different acid or basic solutions for micropaleontologic purposes. This study proposes a new method (DAB), which is based on the consecutive use of acidic and basic solutions to free benthic and planktonic foraminifera from carbonate rocks (argillaceous limestones, marls, phosphatic limestones, chalks) and fine-grained siliciclastics (claystone). It has been successfully employed to prepare micropaleontologic samples from Upper Cretaceous (Maastrichtian) deposits of the Dababiya Quarry Corehole (Upper Nile Valley, Egypt) of which carbonate content varies between 10-80%. The successive use of these solutions yielded good recovery for quantitative analysis but their effects on preservation (i.e. etching) still remains problematic in some cases. Additional heating of solutions provided promising results to reduce the disaggregation time. Processing time may vary depending upon the terrigenous and organic material content for carbonates and claystones. It can be reduced by monitoring the process, or using some other equipments such as a magnetic stirrer.

1.1 Introduction

A firm taxonomic framework is of paramount importance in micropaleontological research and this depends on the recovery of well-preserved microfossils so that their morphologic characters are readily observed. There is little difficulty associated with the extraction of microfossils from deep sea oozes, but it can be extremely difficult to extract them from lithified sediments. Many studies have devised extraction methods of calcareous microfossils (planktonic foraminifera and ostracods) with more or less success. Similar attention has been paid to sediments that are generally difficult to disaggregate.

The procedure described here was carried out on strongly indurated, carbonate-rich rocks and organic-rich siliciclastic lithologies recovered from the Dababiya Quarry Corehole (DQC), which is located in central Egypt, where it was drilled in 2004 (Berggren et al., 2012; fig. 1.1). The 140-meters-thick succession consists of argillaceous limestone with phosphatic limestone intervals, marls, and claystones (fig. 1.2). Additionally, DAB was tested on Paleocene chalk from Shatsky Rise, that contained foraminifera that were still encrusted with sediment following classical micropaleontological procedures.

Two main difficulties arise while working on fine-grained siliciclastics and carbonate rocks for micropaleontologic purposes. The first concerns the recovery of a sufficient number of microfossils to support a reliable interpretation of the data collected. The second is concerned with the recovery of clean microfossils so that the fine morphologic details are visible, permitting correct taxonomic identifications. The aim of this study is to address these difficulties by proposing a technique to extract microfossils from

indurated carbonate rocks and fine-grained sediments without using expensive and/or extremely toxic chemicals such as sodium tetraphenalborate ($NaB(C_6H_5)_4$) (Hantken, 1979), while recovering sufficient amounts of clean specimens for micropaleontologic studies.

1.2 Background

Bourdon (1962) is the first known study that used acetolysis for micropaleontologic purposes. Stouge and Boyce (1983) and later Lethiers and Crasquin-Soleau (1988) also applied acidic solutions for the same purpose (in Lirer, 2000). These authors observed that leaving the samples in an acidic solution for days improved the recovery of microfossils. Hantken (1979) also used a mixture of sodium tetraphenalborate, sodium chloride, and water to extract microfossils from marly shales. Moura et al (1996; 1999) tested the effectiveness of acetolysis by conducting experiments using different concentrations and reported that they obtained good results with 0.5M acetic acid. These authors also emphasized the importance of continuous monitoring during the process to avoid unwanted alteration of microfossil tests. Wanderley (1997) confirmed the effectiveness of this methodology. Lirer (2000) applied 80% dilute acetic acid to lithified carbonates (calcilutites, marly calcilutites, fine-grained calcarenites) and observed that the concentration he applied resulted in clean foraminiferal tests with the processing time being shorter than in Stouge and Boyce (1983). Green (2001) published a handbook in which he explained in great detail sampling techniques, preparation stages specifically adapted to lithologies and organisms. Karimina (2004) promoted dilute acetic acid-based cold disaggregation for extracting calcified radiolaria from micrite nodules. His method

consisted of successive soakings of the rocks, first in 10% dilute HCl and then in 75% acetic acid dilute with 25% of H_2O. Reolid and Herrero (2004) compared the effectiveness of Amine-O, a chemical surfactant, and dilute acetic acid on microfossil extraction from spongiolithic limestone samples from Spain. They concluded that the degree of disaggregation was better in the samples to which acetic acid was applied and pointed out that only low amounts of residue remained after acetolysis. Guray (2006) also faced difficulties in extracting foraminifera from carbonates. After a complete literature review on different techniques, she reached positive results through the use of an acetic acid-chloroform mixture applied for 2 hours. She reported that she obtained identifiable specimens with her method that proved to be superior to methods involving sodium polyphosphate-water solution and calgon-peroxide. Esmeray (2008) also carried out a series of experiments to extract foraminifera from lithified carbonate deposits. She reported that the cleanest specimens were obtained by using a mixture of 50% dilute hydrogen peroxide (H_2O_2) with 50% dilute acetic acid (CH_3COOH). She also recommended using a magnetic stirrer to accelerate the pace of the reaction.

The use of basic solutions would appear to be as effective as that of dilute acids for microfossil extraction. McNeil et al. (2000) heated rock fragments to 70^oC in a bath of Quaternary O, 35% hydrogen peroxide (H_2O_2) and bleach (with 6% sodium hypochlorite) to extract agglutinated foraminifera. These authors reported the recovery of agglutinated foraminifera with excellent preservation. Bice and Norris (2005) made an inspired effort to break down the Cenomanian-Turonian black shales recovered from the Demerara Rise, offshore Suriname, and extracted foraminifera for stable isotope studies. In their study,

they compared the results and effects of calgon-peroxide solution, regular commercial bleach, dishwater detergent, and 100% bleach to determine which of these provided cleaner specimens and still allowed reliable stable isotope studies. They concluded that the use of 100% sodium hypochlorite (NaOCl) yielded the best results.

Remin et al. (2012) applied a different technique to free foraminifera from upper Campaian-lower Maastrichtian chalks and siliceous limestone. They compared the results obtained with liquid nitrogen LN_2 to those obtained with Glauber's Salt method (see Remin et al., 2012 for further explanation) by means of counting the number of specimens recovered and discussed whether conventional methods provided biased results for micropaleontologic interpretations or not.

In all these investigations, researchers used either dilute acidic or basic solutions to obtain cleaner specimens for micropaleontologic purposes. None of these studies involved a method based on the consecutive use of dilute acidic and basic solutions. Therefore, the main objective of this study is to describe a method that is readily applied and affordable, relatively less harmful to the fine test structure of microfossils as well as less hazardous to health than any of the methods cited above.

1.3 Laboratory Procedure

The method described here involves three steps, which are 1) sample preparation, 2) dilute acid processing, and 3) basic solution processing.

1) Regardless of lithology, 10-20 g of rock was crushed into pieces as small as 2-4 mm^3 to increase the surface area to be treated; this was then labeled and weighed. The crushed

sample was dried at ~80^{o}C for 30 minutes to remove moisture in order to avoid the formation of calcium acetate, following the recommendation of Bom et al. (2013). 2) The sample was soaked in 125 ml of 80% dilute acetic acid solution. The exposure times given by Lirer (2000) were the basis for the experiments. The process was not only based on physical observations, but also by monitoring the levels of disaggregation through continuous sampling. These tiny control samples were washed, labeled, and stored separately. These represent negligible amounts of sediment and were not added to the beaker after the control, in case the amount of water retained in clay layers subsequent to washing could affect the concentration of the solution. Once sufficiently disaggregated the sample was washed on a 63μm sieve with lukewarm water, then filtered, labeled and placed in an oven at 80-85^{o}C until it was completely dried. However, a safer approach consisted of drying the samples overnight at lower temperatures (~50^{o}C). 3) The dry sample was then soaked in 125-150 ml 8.25% sodium hypochlorite (commercial bleach) and physical observation along with continuous sampling were repeated until the sample had completely disaggregated. Lastly, the sample was washed, labeled, dried in oven and stored for taxonomic study.

To summarize, this laboratory procedure consists of:

1. Crushing the samples as small as 2 to 4 mm^{3}.

2. Drying in an oven at higher temperatures (70-80^{o}C) for 30 minutes.

3. Soaking in 80% ethanoic acid (Dilute acetic acid).

4. Washing over 63μm sieve with lukewarm water following complete disaggregation.

5. Drying in an oven at high temperatures (70-80^{o}C) for 30 minutes.

6. Soaking the residue in a 8.25% sodium hypochlorite (NaOCl or regular commercial bleach) solution once the sample was completely dried.

7. Washing over 63 μm sieve with lukewarm water.

8. Final drying in an oven at high temperatures (70-80^{o}C) for 30 minutes.

At the completion of this procedure, samples are ready for microscopy and scanning electron microscopy (SEM) imaging of well preserved specimens (fig. 1.3 A-P).

1.4 Processing Time

Experiments were (table 1) initially conducted on 32 samples of marl, 29 of claystone, 27 of argillaceous limestone, 1 of phosphatic limestone, and 1 of chalk. The first tests consisted in applying calgon-peroxide for different durations on two argillaceous limestone samples (sample 6 and 7), in which the carbonate contents were around 75% (fig. 1.4 A). In addition, sonic bathing was applied (fig. 1.4 B). Continuous sampling helped to determine the appropriate duration of the experiments (fig 1.4 C). Splits of same samples also contained the first attempts at using dilute acetic acid (75%; 80%) and soaking in bleach. Figure 1.5 shows the levels of disaggregation under different concentrations. In the light of these results, experiments were successfully carried out on subsequent samples (fig. 1.6).

Another set of experiments was carried out on phosphatic limestone. In DQC two thin phosphatic limestone intervals were present. Only one of these intervals at 82.5 m was available. Figure 7 demonstrates the levels of disaggregation at a sampling interval in 20 minutes.

A series of experiments with different concentrations and additional treatments such as heating and boiling were conducted to extract calcareous microfossils from claystone (appendix 1.1). Heat increases the rate of chemical reactions as observed also by McNeil et al. (2000). Cold acetolysis did not break down claystone and no disintegration was observed even after 24 hours. Subsequently gradual heating and eventually boiling was employed to reduce the processing time. These steps were also repeated with 90% dilute ethanoic acid. Bleach heating (8.25% sodium hypochlorite) was applied in order to lower the duration of the entire process. Different experiments tried are shown in Appendix 1.1.

1.5 Testing the effectiveness of sodium hypochlorite (NaOCl) soaking through time

The sodium hypochlorite treatment was tested separately to determine its effectiveness and the rate of the reaction. Two series of experiments were carried out on an already washed upper Paleocene chalk to define the rate of the reaction. A 0.4 g sample was split by a microsplitter and two sets of time-dependant experiments were conducted. While one half was immersed for an hour, the other half was washed every 15 minutes.

1.6 Reaction mechanism

H^+ ion releasing capacity of acids to the solution under certain levels of pressure and temperature defines the acidity of the mixture. Acetic acid is a weak acid due to its low levels of H^+ ion releasing capacity. H^+ ions remain bounded to the H_3C_2OOH or CH_3COOH^- molecule whereas acids such as hydrogen peroxide (H_2O_2), hydrochloric acid (HCl), and hydrofluoric acid (HF) are more corrosive since the quantities of the H^+ they release to the solution are higher than the acetic acid. Therefore, the reaction to

acetic acid occurs slower than other acids. Bom et al. (2013) explained the reaction as below:

$$\mathbf{CH_3COOH_{(aq)} + H_2O \rightarrow CH_3COO^- + H_3O^+_{(aq)}} \quad \mathbf{[1]}$$

Moura et al. (1999) explained the rationale behind the use of acidic solutions. They stated that good preservation of calcareous microfossils lies in the purity differences between the foraminifera tests and the matrix of sediments. The purer the chemistry is, the more resistant it is to the corrosive effects of these solutions. Therefore, the disaggregation of the matrix occurs faster that of the calcareous test itself (fig. 1.10). Even if acidic soaking cannot break up the lithology, it preferably creates weakness zones between foraminifera and lithology.

The use of calgon-peroxide or calgon solutions is a widely employed, whereas, that of basic solutions is not. The main idea behind the use of sodium hypochlorite is the production of sodium carbonate, during the process. Equation 2 is the proposed reaction equation of sodium hypochlorite with calcium carbonate that explains the main idea of using this solution.

$$\mathbf{2NaOCl + CaCO_3 \leftrightarrow Na_2CO_3 + CaCl_2 + O_2} \quad \mathbf{[2]}$$

After acetolysis, weakness zones become more prominent. Sodium hypochlorite preferably attacks where the test of foraminifera and carbonate rock intersects just as dilute acetic acid does. The formation of sodium carbonate (Na_2CO_3), which accelerates relatively harmless disaggregation, will slowly begin being accumulated along the

weakness zone of test and rock. I can only speculate that the presence of calcium chloride ($CaCl_2$) causes the excessive etching of calcareous microfossils because its effects on calcareous tests are unknown yet. The side effects of trace amounts of chemical compounds in bleach on foraminifera tests and ostracoda carapaces is still unclear. The properties of these chemicals are beyond the scope of this research and will be the subject of future research.

1.7 Discussion

Nine points are discussed 1) Size heterogeneity of the crushed sample, 2) duration of the process, 3) use of solution in sufficient amounts, 4) solution concentration, 5) additional applications, 6) effects of overexposure 7) the amount of residue and 8) cost efficiency and 9) unknown side effects.

1) Crushing increases the effectiveness of the treatment by increasing the surface area in contact with the solution. Consequently, heterogeneity of crushed samples should be avoided. Although not used in this study, sieving after crushing might be a useful procedure that would ensure a more homohenous size fraction. I recommend crushing samples to pieces as small as 1-5 mm^3.

2) I essentially followed the timing given by Lirer (2000). Some samples required disaggregation times that were longer than proposed. However, for some carbonate rocks the acid concentrations he proposed yielded good results. The differences in the quality of the results are most likely due to difference in rock properties such as

carbonate/terrigenous ratio, permeability, porosity, degree of diagenesis and diagenetic alteration, terrigenous material type, etc. Although it is more time consuming than methods involving H_2O_2 or HF and other chemicals, DAB allows better control on disaggregation. Considering all experimental results (appendix 1.1), the required processing time (table 2) for argillaceous limestone is 5-6 hours with cold acetolysis, and 4-5 hours with applied heated acetolysis. The subsequent bleach treatment requires 3 to 4 hours cold soaking or 2 to 3 hours soaking with heating. For the disintegration of phosphatic limestone 2-2.5 hours of cold ethanoic acid soaking yields good results. Subsequent bleach soaking for 45 minutes to 1 hour would result in clean microfossils. For already-washed chalks 1 to 1.5 hours of cold bleach treatment or about 1 hour of heated bleach treatment will be sufficient to obtain good specimens. Physical observation and continuous sampling should be regularly performed. Ethanoic acid solution with 90% concentration and subsequent bleach soaking should be used for lithologies such as claystone, mudstone and shale; boiling during both treatments is necessary to break down these rocks. Required time is between 5 and 7.5 hours for acidic and 4 to 6 hours for bleach soaking.

3) Lirer (2000) emphasized the need to cover the crushed sample with a minimum of 2 cm of solution. Although all samples were covered with more than 2 cm of solution at the beginning of the treatment a few samples completely absorbed the solution. If insufficient amounts of solution are used, the samples become exposed to the atmospheric effects, which may result in the destruction of the fine structure and the ornamentation of the test. Physical and chemical properties of acetic acid, additional applications such as heating

and boiling, terrigenous material type, organic-material content, permeability, and porosity of the sediment may be responsible for the drying out of the upper part of the sample. I suggest 125 ml (or not less than 100 ml) solution for 10-20 g of crushed sample regardless of lithology and related physical and chemical properties.

4) Some researchers used solutions with different concentrations (Stouge and Boyce, 1983; Karimina, 2004). Here I experimented as follows 1) I changed the concentration during a treatment; and 2) I experimented at different concentrations. Changing the concentration adds one more variable to the complex procedure and affects the rate of the chemical reaction and therefore, the procedural time. The effect of different concentrations should be carefully controlled through continuous sampling and side-by-side experiments.

5) I tested the effects of heating and boiling of acidic and basic solutions on speed and quality of disaggregation. Although more experiments are required clear results will be obtained (appendix 1.1).

6) Moura et al. (1999) stated that overexposure to the acids resulted in dissolved tests that hampered correct taxonomic identification. Hodgkinson (1991) noted that some researchers observed translucency, fragility and etching on scolecodonts and foraminifera as a result of using 8-12% chlorine containing bleach treatment. This study confirms that overexposure resulted in translucency (fig. 1.8) and etching (fig. 1.3C).

7) Reolid and Herrero (2004) stated that the recovery of microfossil was significantly dependant on the weight of the processed sample. This study confirms this relationship in showing that for approximately 10-20 g crushed sediment, the recovered residue never exceeded 1g. Therefore, studies requiring more than 1g sediment should be based on using more than 10-20 g sample.

8) A major benefit of this methodology is its cost efficiency. Compared to the methods requiring the use of liquid nitrogene or sodium tetraphenalborate, which are expensive and difficult to handle. DAB, in contrast, promotes uses of chemicals that are affordable, broadly available, and easy to handle.

9) During the first experiments of acidic soaking, I observed differences between the splits of one limestone sample (fig. 1.5 B and C) so that one split contained excessively sulphidized tests and unidentifiable grains. This may be due to the chemical induction or reduction of clay minerals under experimental acidic conditions. No other limestone samples produced similar anomalous contents. This sulphidication might be one of the unknown side effects of the DAB.

1.8 Warning

As stated in previous studies, taking appropriate measures such as wearing lab shirts, gloves, goggles, and masks during laboratory work in essential. Also overexposure to hazardous chemicals may be cumulative in the human body and may cause or trigger diseases.

With this study, I invite researchers to conduct experiments to improve this new methodology, and also I would like to be informed about the its weaknesses.

1.9 Acknowledgements

The author gratefully acknowledges his scholarship providing institution TPAO (Türkiye Petrolleri Anonim Ortaklığı, Ankara, TURKEY) and thesis advisors Professors Marie-Pierre Aubry, William A. Berggren and Richard K. Olsson for their constructive comments, sharing their experiences and discussions about the use of different methods and chemicals. I would like to thank to Dr. Christopher King (Dorset, UK) and Dr. Nageh Obaidalla (University of Assiut, Egypt) for their recommendations on the procedures to follow and Dr. David Bord, Weimin Si, Rehab Salem and Tarek Salem for helping with literature research.

1.10 References

Berggren, W.A., Alegret, L., Aubry, M-P., Cramer, B.S., Dupuis, C., Goolaerts, S., Kent, D.V., King, C., Knox, R.W.O'B., Obaidalla, N., Ortiz, S., Ouda, K.A.K., Abdel-Sabour, A., Salem, R., Senosy, M.M., Soliman, M.F., Soliman, A., 2012. The Dababiya Corehole, Upper Nile Valley, Egypt: Preliminary results. Austrian Journal of Earth Sciences, vol. 105/1, 161-168.

Bice, K.L., Norris, R.D., 2005. Data report: Stable isotope ratios of foraminifers from ODP Leg 207, Sites 1257, 1258, and 1260, and a cleaning procedure for foraminifers in organic-rich shales. *In* Mosher, D.C., Erbacher, J., and Malone, M.J. (Eds.), *Proc. ODP, Sci. Results*, 207 [Online]. Available from World Wide Web: <http://www- odp.tamu.edu/publications/207_SR/104/104.htm>.

Bom, M.H.H., Kochhann, K.G.D., Rodrigues , G.B., Fauth, G., 2013. Acetic acid in micropaleontology: Its efficiency in disaggregating carbonate rocks and recovering calcareous and siliceous microfossils. Acetic acids chemical properties, production and applications. Nova Science Publishers, New York, ISBN: 978-1-62948-222-4.

Bourdon, M., 1962. Methode de degagement des microfossiles par acetolyse a chaud. Compte Rendu Sommaire des Séances de la Société Géologique de France, p. 267-268.

Esmeray, S., 2008. Cretaceous/Paleogene boundary in the Haymana Basin, Central Anatolia, Turkey: Micropaleontological, Mineralogical and Sequence Stratigraphic Approach. [M.Sc. Thesis]: Middle East Technical University, Turkey.

Green, R.O., 2001. A manual of practical laboratory and field techniques in paleobiology. Kluwer Academic Publishers. ISBN 978-90-481-4013-8.

Guray, A., 2006. Campanian-Maastrichtian planktonic foraminiferal investigation and biostratigraphy (Kokaksu Section, Bartin, NW Anatolia): Remarks on the Cretaceous paleoceanography based on quantitative data. [M.Sc. Thesis]: Middle East Technical University, Turkey.

Hantken, N-M, 1979. The use of Sodium Tetraphenalborate and Sodium Chloride in the extraction of fossils from shales. Journal of Paleontology. 53 (3).

Hodgkinson, R.L., 1991. Microfossil processing: a damage report. Micropaleontology, vol. 37, no. 3, pp. 320-326.

Karimina, S.M., 2004. Extraction of calcified Radiolaria and other calcified microfossils from micritic limestone utilizing acetic acid. Micropaleontology. Vol. 50, no. 3, p 301-306.

Lethiers, F., Crasquin-Soleau, S., 1988. Comment extraire les microfossiles a' tests calcitiques des roches calcaires dures. Revue de Micropaleontologie, 31(1):56-61.

Lirer, F., 2000. A new technique for retrieving calcareous microfossils from lithified lime deposits. Micropaleontology, v. 46, p. 365-369.

McNeil, D.H., Leckie, D.A., Kjarsgaard, B.A., Stasiuk, L.D., 2000. Agglutinated foraminiferal assemblages in Albian shales overlying kimberlite deposits in the Smeaton core from central Saskatchewan, Canada. *In*: Hart, M.B., Kaminski, M.A., & Smart, C.W., (eds). Proceedings of the Fifth International Workshop on Agglutinated Foraminifera. Gryzbowski Foundation Special Publication, No. 7, 299-309.

Moura, J.C., Sousa, F.P., Wanderley, M.D., Rios-Netto, A.M., 1996. Um método alternativo para extração de microfósseis carbonáticos de rochas calcárias, com emprego de ácidos diluídos e tempo de exposição controlado. Anales do XXXXIX Congresso Brasileiro de Geologia 2, 273–275.

Moura, J.C., Rios-Netto, A.M., Wanderley, M.D., Sousa, F.P., 1999. Using acids to extract microfossils from carbonate rocks. Micropaleontology, vol 45, no. 4, pp. 429-436.

Remin, Z., Dubicka, Z., Kozlowska, A., Kuchta, B., 2012. A new method of rock disintegration and foraminiferal extraction with the use of liquid nitrogen [LN_2]. Do conventional methods lead to biased paleoecological and paleoenvironmental interpretations?. Marine Micropaleontology. 86-87, pp. 11-14.

Reolid, M., Herrero, C., 2004. Evaluation of methods for retrieving foraminifera from indurated carbonates: application to the Jurassic spongiolithic limestone lithofacies of the Prebetic Zone (South Spain). Micropaleontology, vol 50, no. 3, pp. 307-312.

Soudry, D., Glenn, C.R., Nathan, Y., Segal, I. and VonderHaar, D., 2006. Evolution of Tethyan phosphogenesis along the northern edges of the Arabian-African shield during the Cretaceous-Eocene as deduced from temporal variations of Ca and Nd isotoped and rates of P accumulation. Earth-Science Reviews, 78:27-57.

Stouge, S., Boyce, W.D., 1983. Fossils of Northwestern Newfoundland and Southeastern Labrador: Conodonts and Trilobites. Mineral Development Division Department of Mines Energy Government of Newfoundland and Labrador. ST. John's Newfoundland - Report 83-3.

Tur, N.A., Smirnov, J.P., Huber, B.T., 2001. Late Albian-Coniacian planktonic foraminifera and biostratigraphy of the northeastern Caucasus. Cretaceous Research, 22: 719-734.

Wanderley, M.D., 1997. Estudo de uma secao cretacica da Bacia Potiguar com base en nanofosseis calcarios. Rio de Janerio: Universidade Federal do Rio de Janerio. Depto. De Geologia (Unpublished dissertation).

1.11 Figure Captions

Figures:

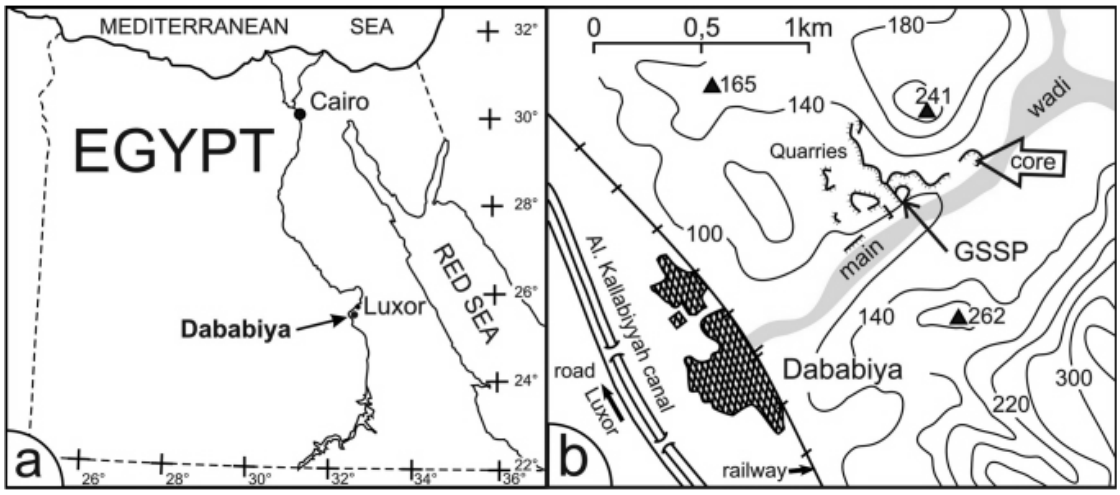

Figure 1.1

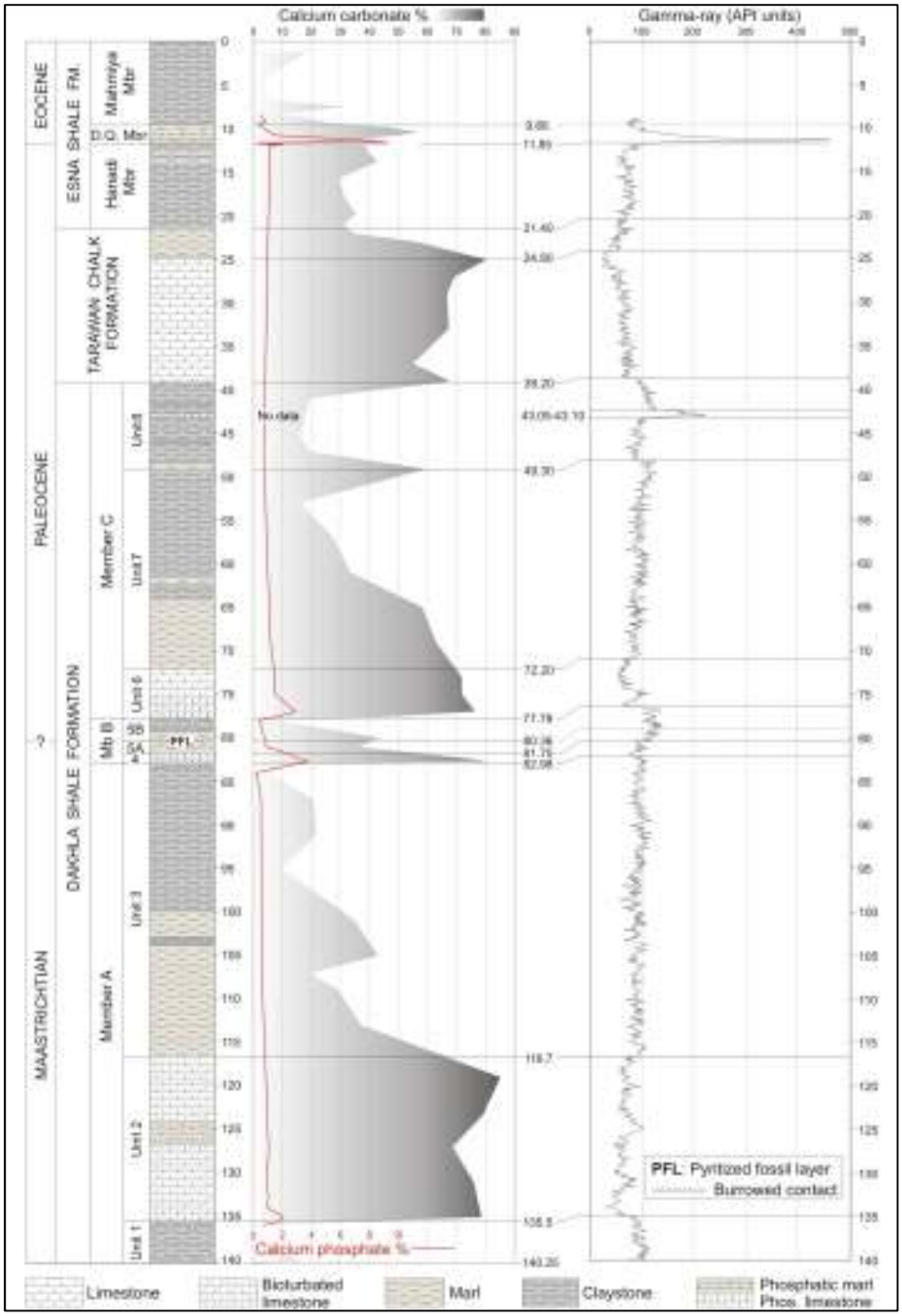
Calcium carbonate %
Gamma-ray (API units)
EOCENE
PALEOCENE
MAASTRICHTIAN
ESNA SHALE FM.
TARAWAN CHALK FORMATION
DAKHLA SHALE FORMATION
Mahmiya Mbr
Hanadi Mbr
Member C
Member A
Unit8
Unit7
Unit6
Unit3
Unit2
Unit1
Mb B
PFL
No data
9.66
11.89
21.40
24.50
39.20
43.05-43.10
49.30
72.20
77.79
80.38
81.75
82.98
118.7
135.5
140.20
Calcium phosphate %
PFL: Pyritized fossil layer
Burrowed contact
Limestone
Bioturbated limestone
Marl
Claystone
Phosphatic marl
Phos. limestone

Figure 1.2

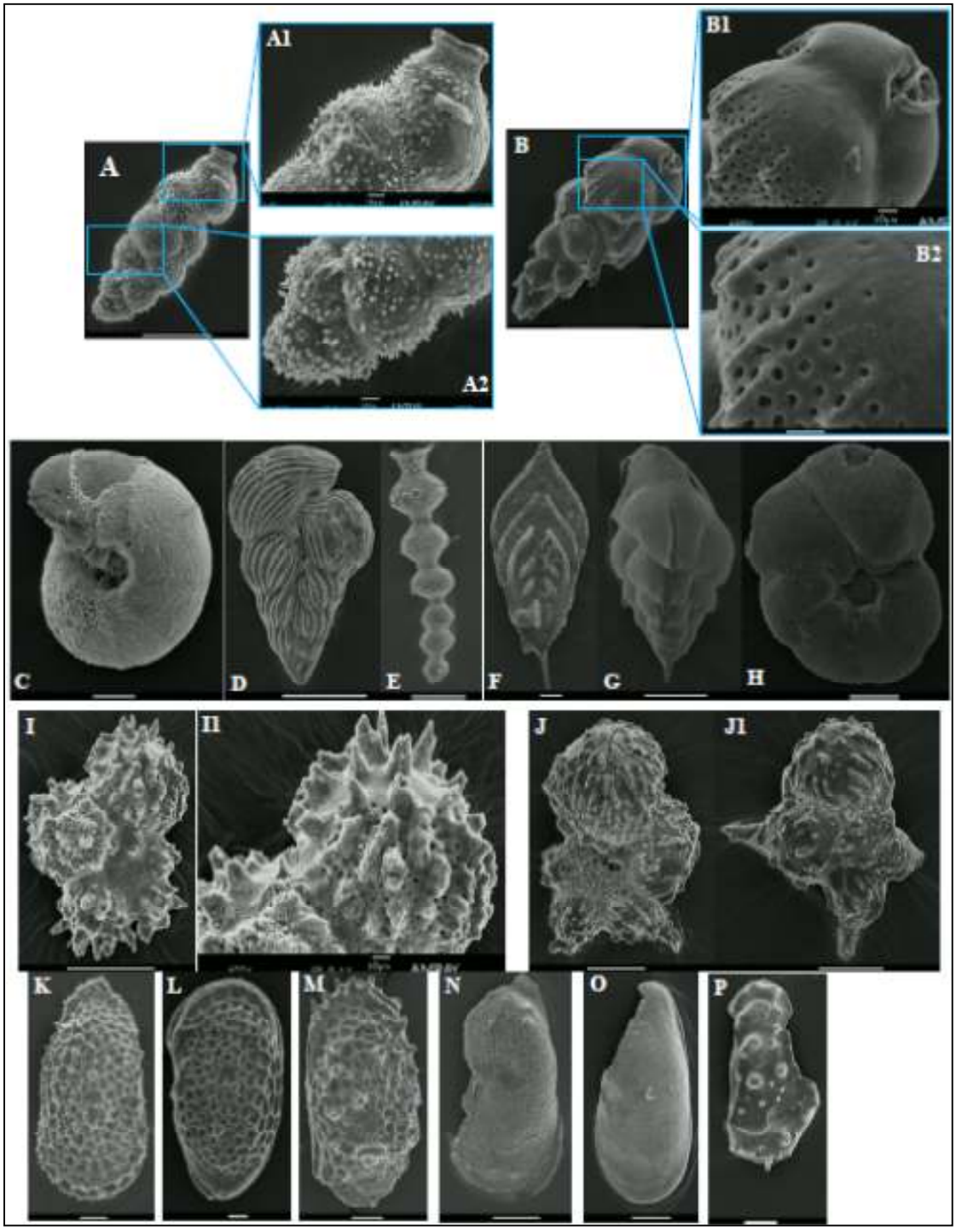

Figure 1.3

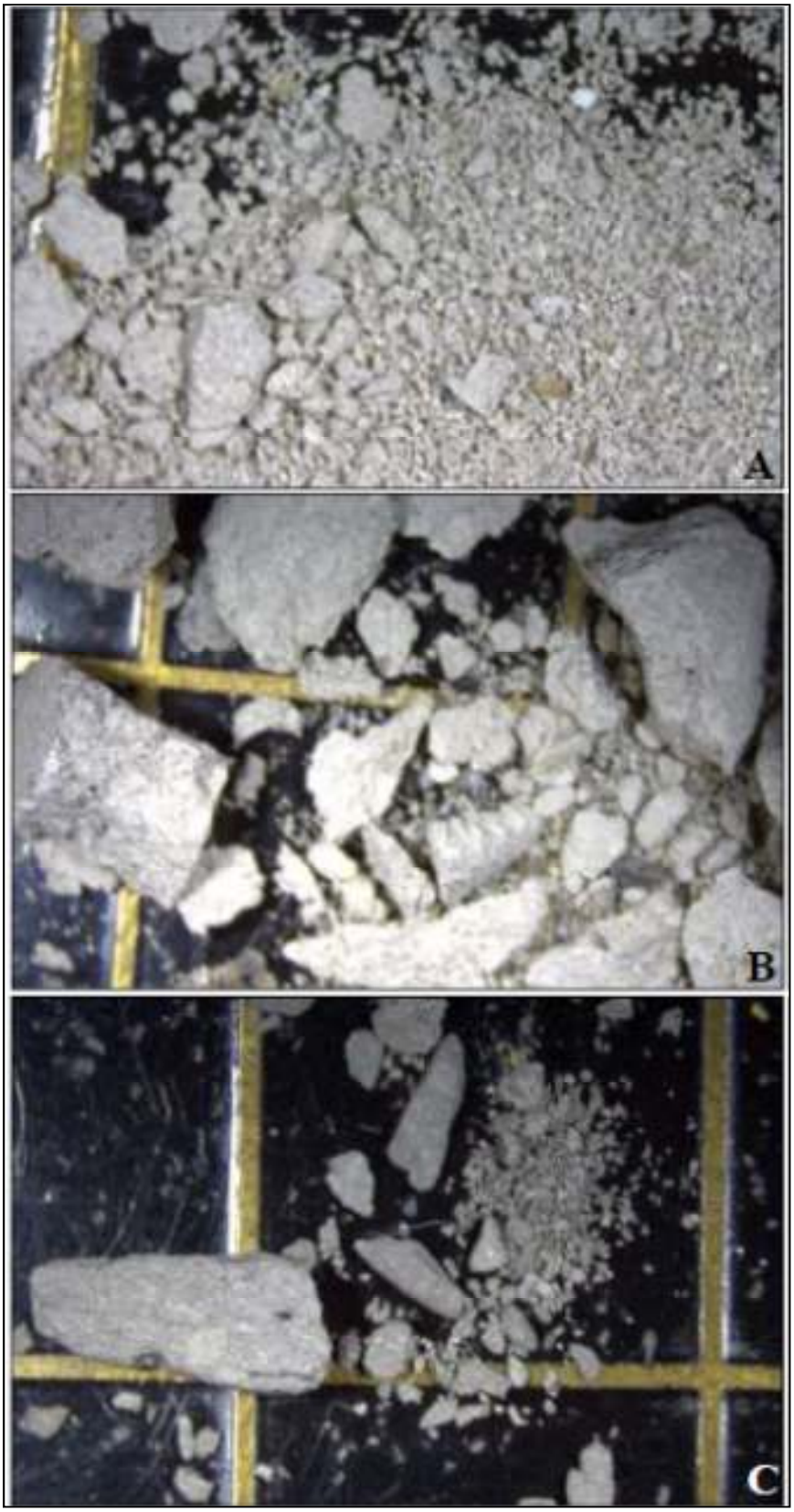

Figure 1.4

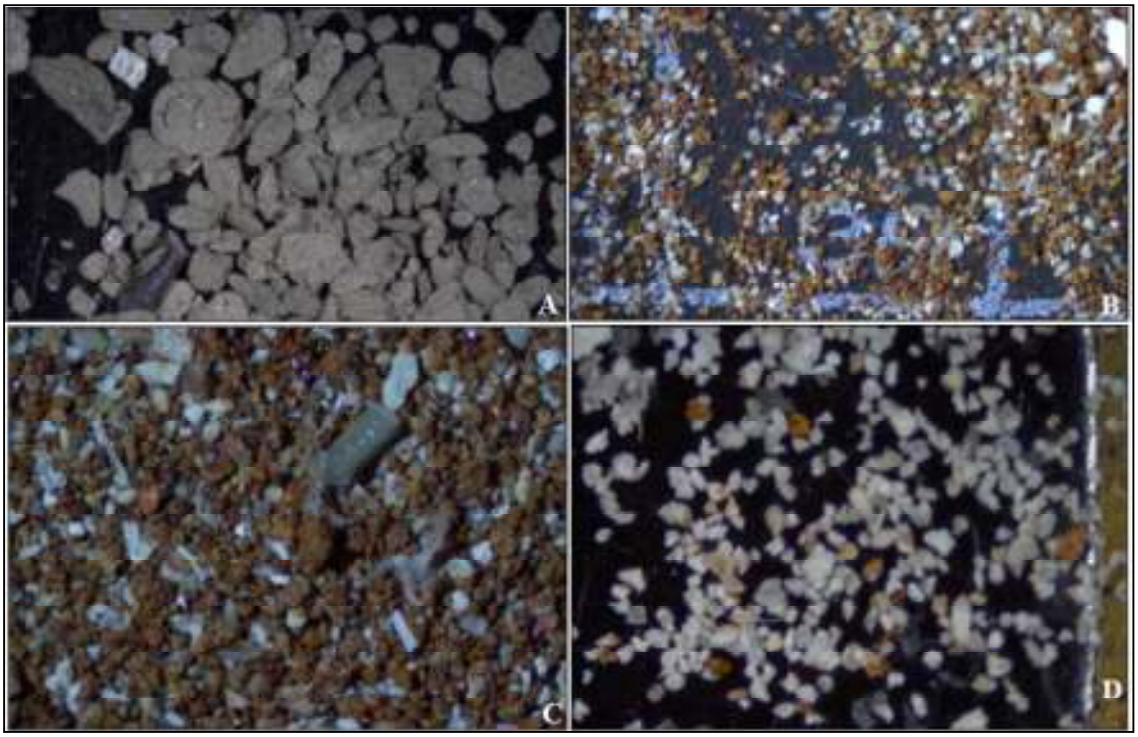

Figure 1.5

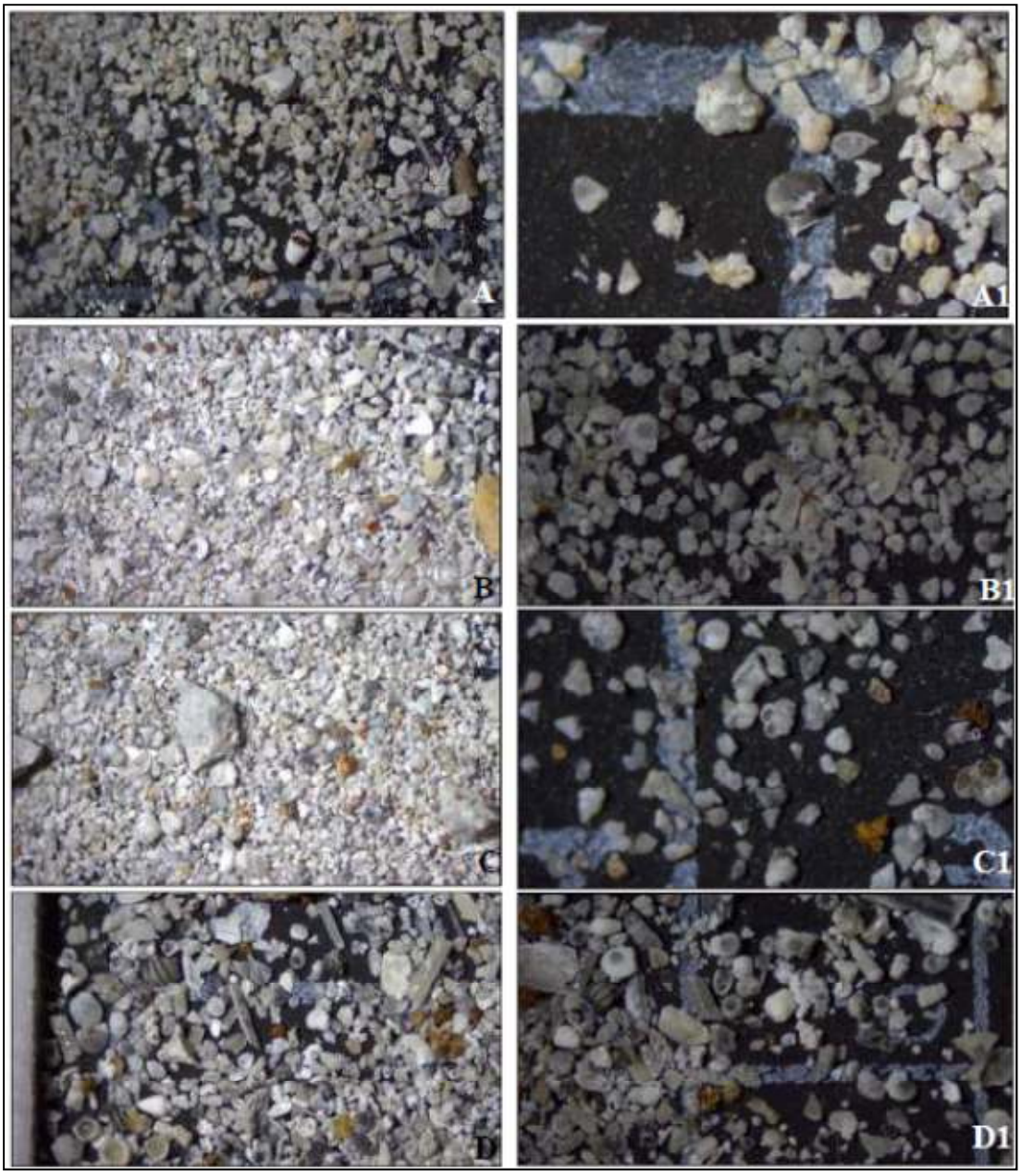

Figure 1.6

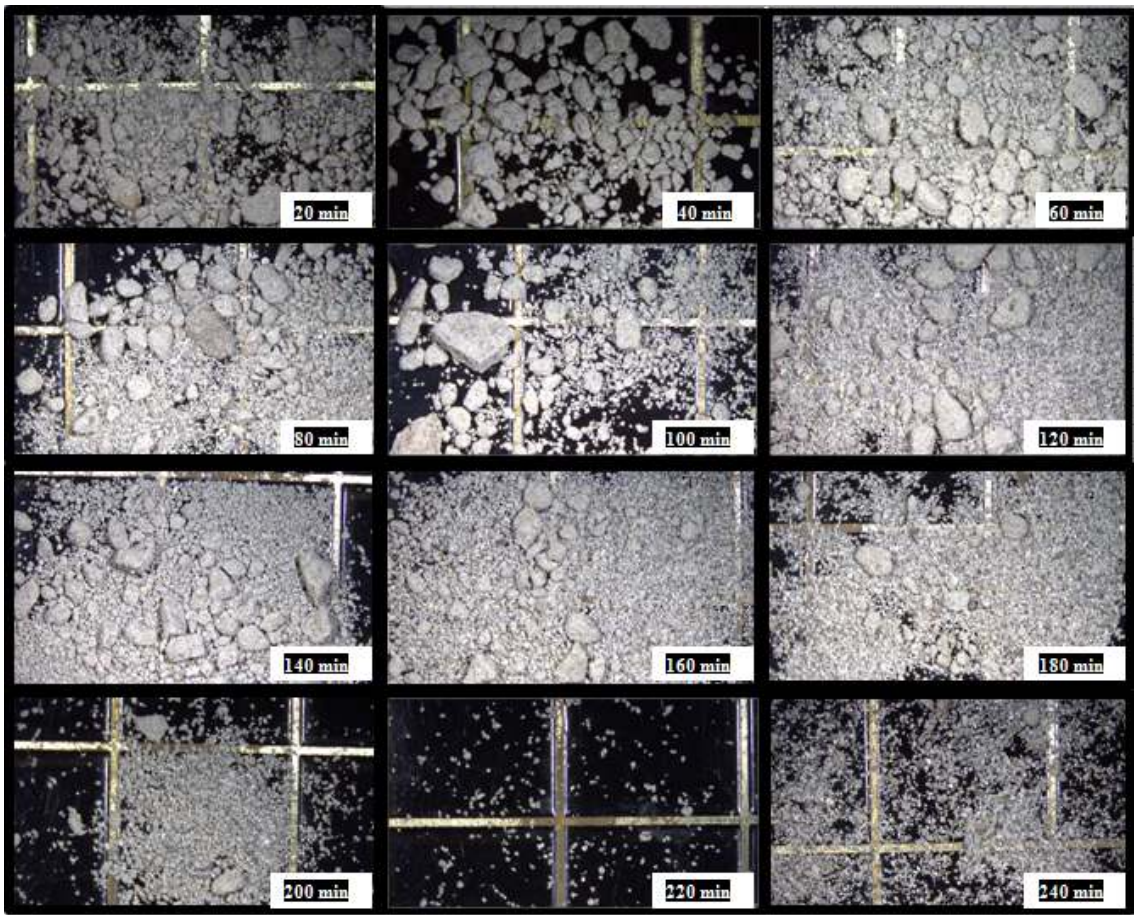
20 min
40 min
60 min
80 min
100 min
120 min
140 min
160 min
180 min
200 min
220 min
240 min

Figure 1.7

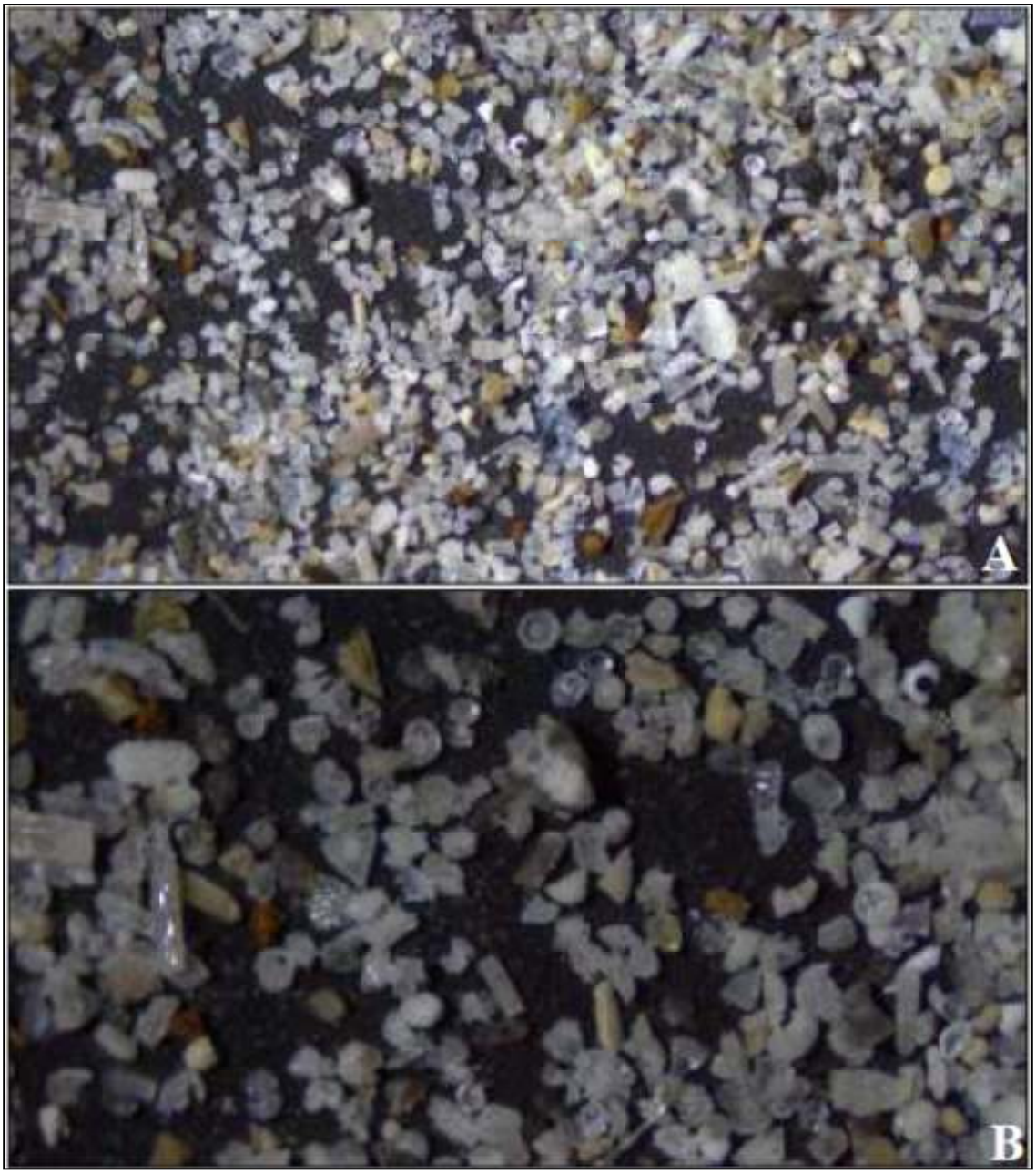

Figure 1.8

Figure 1.9

Table 1.1

Sample No	Depth (m)	Lithology
#1	139.87-88	Claystone
#2	139.5	Claystone
#3	138.5	Claystone
#4	137.5	Claystone
#5	136.3	Claystone
#6	134.5	Arg. Lime
#7	133.25-.27	Arg. Lime
#8	132.5	Arg. Lime
#9	131.51-.49	Arg. Lime
#10	131-130.98	Arg. Lime
#11	130.47-.51	Arg. Lime
#12	129.47-.50	Arg. Lime
#13	128.1	Arg. Lime
#14	127.18-20	Arg. Lime
#15	126.40-.42	Marl
#16	125.55-.57	Marl
#17	124.91-.93	Marl
#18	124.17-.19	Marl
#19	123.5	Arg. Lime
#20	122.5	Arg. Lime
#21	121.88-.90	Arg. Lime
#22	121.25	Arg. Lime
#23	120.18-.2	Arg. Lime
#24	119.6	Arg. Lime

Sample No	Depth (m)	Lithology
#25	118.65-.67	Arg. Lime
#26	118.10-12	Arg. Lime
#27	117.2	Arg. Lime
#28	116.40-.45	Marl
#29	115.15	Marl
#30	114.47-50	Marl
#31	113.19	Marl
#32	111.91	Marl
#33	111.4	Marl
#34	111.09-10	Marl
#35	110.5	Marl
#36	109.22	Marl
#37	108.5	Marl
#38	107.46	Marl
#39	106.5	Marl
#40	105.89	Claystone
#41	104.32-.34	Marl
#42	103.63	Claystone
#43	102.5	Marl
#44	101.5	Marl
#45	100.55-.57	Marl
#46	99.8	Claystone
#47	98.5	Claystone
#48	97.72	Claystone
#49	97.2	Claystone
#50	96.5	Claystone
#51	95.5	Claystone
#52	94.25-.22	Claystone
#53	93.5	Claystone
#54	92.5-.48	Claystone
#55	91.5	Claystone
#56	90.89-.88	Claystone
#57	90.09	Claystone
#58	88.70-.68	Claystone
#59	87.47	Claystone
#60	86.45-.42	Claystone
#61	85.55	Claystone
#62	84.55-.52	Claystone
#63	83.75-.73	Claystone
#64	83.15	Claystone

Sample No	Depth (m)	Lithology
#65	82.5	**Phos lime**
#66	81.05-.02	Marl
#67	80.47-.46	Marl
#68	80.44-.43	Marl
#69	80.4-.39	Marl
#70	80.39-.38	Marl
#71	80.38-.37	Marl
#72	80.34-.32	Marl
#73	79.93-.91	Marl
#74	79.5	Claystone
#75	78.5	Claystone
#76	77.82	Claystone
#77	77.7	Arg. Lime
#78	76.5	Arg. Lime
#79	75.72-.70	Arg. Lime
#80	75.6	Arg. Lime
#81	74.45	Arg. Lime
#82	73.63-.61	Arg. Lime
#83	73.25	Arg. Lime
#84	72.45	Arg. Lime
#85	72.03-72	Arg. Lime
#86	71.5	Marl
#87	70.6	Marl
#88	70.02-.70	Marl
#89	69.47-.45	Marl
#90	ODP 198/1209A/024/126-127	**Chalk**

Table 1.1 ends.

Table 1.2

Lithology	**Acid Concentration (%)**	**Duration (Hours) (*Acidic*)**	**Duration (Hours) (*Basic*)**
Argillaceous limestone & Marl	80	3-5 (Cold) 4-5 (Heated)	4-5 (Cold) 2-3 (Heated)
Phosphatic limestone	80	2-2.5 (Cold)	3/4-1 (Heated)
Chalk	80	Not tested	1-1.5 (Cold) 3/4-1 (Heated)
Claystone, Mudstone, Shale	90	5-7.5 (Heating/Boiling)	4-6 (Heating/Boiling)

Appendix 1.1

Lithology	Sample ID	Acid %	Duration (Hours)	App.	Basic	Duration (Hours)	App.	Extra Acidic	Extra Basic	Additional
Marl	106.5	80	3h	Cold	+	5h3m	Cold	-	-	-
Claystone	105.89	80	3h15m	Cold	+	5h7m	Cold	-	-	-
Marl	104.32-.34	80	3h15m	Cold	+	5h12m	Cold	-	-	-
Claystone	103.63	80	5h6m	Cold	+	5h31m	Cold	-	-	-
Marl	102.5	80	5h6m	Cold	+	5h37m	Cold	-	-	-
Marl	101.5	80	5h6m	Cold	+	5h39m	Cold	-	-	-
Marl	100.55-.57	80	5h6m	Cold	+	5h43m	Cold	-	-	-
Claystone	99.8	80	5h	Boiling	-	-	-	-	-	-
Claystone	98.5	80	5h7m	Boiling	-	-	-	7.5h 80% Hot (~100ºC)	4h40m Cold	-
Claystone	97.72	80	5h15m	Boiling	-	-	-	7.5h 80% Hot (~100ºC)	4h43m Hot (~100ºC)	-
Claystone	97.2	80	5h	Boiling	-	-	-	8h28m 90% Hot (~100ºC)	4h40m Hot (~100ºC)	-
Claystone	96.5	80	5h7m	Boiling	-	-	-	8h17m 90% Hot (~100ºC)	4h40m Hot (~100ºC)	-
Claystone	95.5	80	5h13m	Boiling	-	-	-	8h21m 90% Boiling	4h46m Boiling	4h44min Bleach Boiling
Claystone	94.25-.22	80	5h	Boiling	-	-	-	8h25m 90% Boiling	4h51m Boiling	3h39min Bleach Boiling
Claystone	93.5	80	5h6m	Boiling	-	-	-	7h46m 90% Boiling	4h51m Boiling	3h42min Bleach Boiling

Lithology	Sample ID	Acid %	Duration (Hours)	App.	Basic	Duration (Hours)	App.	Extra Acidic	Extra Basic	Additional
Claystone	92.5-.48	80	5h12m	Boiling	-	-	-	7h44m 90% Boiling	4h52m Boiling	4h46min Bleach Boiling
Claystone	91.5	80	5h	Boiling	-	-	-	7h48m 90% Boiling	4h53m Boiling	3h Bleach Boiling
Claystone	90.89-.88	80	5h7m	Boiling	-	-	-	7.5h 90% Boiling	4h44m Boiling	2h34min Bleach Boiling
Claystone	90.09	80	5h16m	Boiling	-	-	-	7h34m 90% Boiling	4h45m Boiling	3h Bleach Boiling
Claystone	88.70-.68	90	7.5h	Boiling	+	4h44m	Boil	7.5h 90% Boiling	4h44m Boiling	2h31min Bleach Boiling
Claystone	87.47	90	7h34m	Boiling	+	4h21m	Boil	7h34min 90% Boiling	4h21m Boiling	2h26min Bleach Boiling
Claystone	86.45-.42	90	7.5h	Boiling	+	4h	Boil	7.5h 90% Boiling	4h Boiling	2h39min Bleach Boiling
Claystone	85.55	90	7h	Boiling	+	4h40m	Boil	-	2h7min Bleach Boiling	-
Claystone	84.55-.52	90	7h	Boiling	+	6.5h	Boil	-	2h6min Bleach Boiling	-
Claystone	83.75-.73	90	7h	Boiling	+	5h5m	Boil	-	4h Bleach (Cold)	-
Claystone	83.15	90	7h	Boiling	+	5h7m	Boil	-	-	-
Marl	81.05-.02	90	5h49m	Cold	+	2h44m	Cold	-	-	-

Lithology	Sample ID	Acid %	Duration (Hours)	App.	Basic	Duration (Hours)	App.	Extra Acidic	Extra Basic	Additional
Claystone	79.5	90	7h	Boiling	+	6h24m	Boil	5h13min90% Boiling	-	-
Claystone	78.5	90	7h	Boiling	+	6h37m	Boil	5h18min90% Boiling	-	-
Claystone	77.82	90	7h	Boiling	+	6h38m	Boil	58min 90% Boiling	2h1min Bleach Boiling	-
Arg. Lime	77.7	80	5h19m	Boiling	+	1h2m	Cold	-	-	-
Arg. Lime	76.5	80	5h7m	Boiling	+	1h3m	Cold	-	-	-
Arg. Lime	75.72-.70	80	5h27m	Boiling	+	1h11m	Cold	-	-	-
Arg. Lime	75.6	80	4h45m	Boiling	+	1h19m	Boil	-	-	-
Arg. Lime	74.45	80	5.5h	Boiling	+	56m	Cold	-	-	-
Arg. Lime	73.63-.61	80	5h6m	Boiling	+	1h9m	Cold	-	-	-
Arg. Lime	73.25	80	4h53m	Boiling	+	1h14m	Boil	-	-	-
Arg. Lime	72.45	80	4h13m	Boiling	+	1h34m	Cold	-	-	-
Arg. L.	72.03-72	80	4h35m	Boiling	+	1h18m	Boil	-	-	-
Marl	71.5	80	4h8m	Boiling	+	1h32m	Cold	-	-	-
Marl	70.6	80	5h9m	Boiling	+	52m	Cold	-	-	-

Appendix 1.1 ends.

CHAPTER 2

Upper Campanian(?) to Lower Danian Planktonic Foraminiferal Biostratigraphy of the Dababiya Quarry Corehole, Upper Nile Valley, Egypt

Fırat GÖÇMENOĞLU[1,2]

1) Department of Earth & Planetary Sciences, Rutgers, The State University of New Jersey
Wright-Rieman Laboratories, 610 Taylor Road.,
Piscataway, NJ 08854-8066

2) Türkiye Petrolleri Anonim Ortaklığı (TPAO)*, Araştırma Daire Başkanlığı*
Söğütözü Mahallesi, 2180. Cadde, No.10
06100 Çankaya-Ankara/TÜRKİYE.

Abstract

This study establishes an upper Campanian(?) to lower Danian planktonic foraminiferal biostratigraphy for the lower six units of the Dakhla Shale Formation (DSF) recovered from the Dababiya Quarry Corehole (DQC) and discusses the location of the K/Pg boundary. The section extends from the upper Campanian(?) *Globotruncana aegyptiaca* lowest occurrence zones (LOZ) at the bottom of the core to the base of the lower Danian Pα *Parvularugoglobigerina eugubina* Total Range Zone (TRZ) at 75.72 m. I used a combined the biostratigraphic scheme of Caron (1985) and Li and Keller (1998) to establish a biostratigraphic subdivision of the section. Planktonic foraminiferal and calcareous nannoplankton datum levels were used to evaluate the temporal continuity of the section. The ?upper Campanian- Maastrichtian section appears to be continuous and to extend uninterrupted into the lower Danian. There is probably a short hiatus at ~79 m spanning Zone NP1 (partim) and NP2 (partim). In addition, the reliability of pseudoguembelininds in biostratigraphy is discussed.

2.1 Introduction

The 140 m Dababiya Quarry Corehole (DQC) is located about 35 km south of Luxor, Upper Nile Valley (fig. 2.1a), on the stable shelf area of North Africa (Youssef, 2003). It spans the stratigraphic interval from Campanian(?) to lower Eocene, and was drilled to recover well-preserved sediments in the vicinity of the GSSP for the Paleocene/Eocene Series boundary, which was defined in the adjacent quarry outcrop (Aubry et al., 2007) (fig. 2.1b). Lithostratigraphic units of the core are in ascending order: Dakhla Shale Formation (DSF), Tarawan Chalk Formation (TCF), Esna Shale Formation (ESF) (see Dupuis and Knox, 2012 for detailed explanation). Berggren et al. (2012) informally subdivided DSF into three members and nine units (fig. 2.2).

Alegret and Ortiz (2012), Aubry and Salem (2012a, b), Gooalerts and Dupuis (2012), Obaidalla (2012), Ouda et al. (2012) provided macro- and micropaleontologic, and biostratigraphic results of the DQC. Aubry and Salem (2012a) located the Cretaceous/Paleogene (K/Pg) boundary between 80.40 and 80.20 meters in DQC based on the nannoplankton biostratigraphy, whereas Obaidalla (2012) interpreted the section as being discontinuous at the K/Pg boundary.

This study attempts to: 1) provide a planktonic foraminiferal biostratigraphy for the DSF unit 1 to unit 6 (partim); 2) locate the K/Pg boundary based on planktonic foraminiferal biostratigraphy; 3) evaluate the continuity of the section through the analysis of the sedimentation rate (SR) plot by combining nannoplankton and planktonic foraminiferal

biostratigraphy and 4) discuss the reliability of biostratigraphic markers from a paleoenvironmental perspective.

2.2 Material and Methods

2.2.1 Material

The Dababiya Quarry corehole consists of 140 meters of Upper Cretaceous to Lower Eocene mudstones and limestones that are assigned to the Dakhla Shale Formation (DSF), Tarawan Chalk Formation (TCF) and Esna Shale Formation (ESF) (Berggren et al., 2012). The DSF was divided into three members informally named A, B and C, in stratigraphic order (fig. 2.2). Member A consists of claystone, limestone, and marl and was divided into three units. Unit-1 (140.25-135.50 meters) consists of claystones with an increasing carbonate content upwards. Its thickness is 5.25 meters. Unit-2 (135.50-116.40 m) unconformably overlies unit-1 with a thin phosphatic limestone marking its base. This 18.80 meter thick unit consists of intensively bioturbated limestone, interrupted by a 2.65 meters thick (126.65-124.00 m) light medium gray calcareous marly interval. The 33.42 meters thick unit-3 (116.40-82.98 m) consists of marl and claystone. In the upper part of the marls there is a thin claystone interval (104.0-103.0 m). A thicker claystone extends from 99.80-82.98 m in the upper part of the unit.

Member B consists of phosphatic limestone, marl, and claystone. It was divided into three units (4, 5A and 5B). Unit-4, which is 1.23 meters thick, consists of phosphatic limestones. Unit-5A consists of medium gray calcareous marls. Dupuis and Knox (2012) used a thin pyritized fossil layer (PFL) at 80.36 m to mark the boundary between units

5A and 5B. Unit-5B (80.36-77.78 m) begins with marls and changes to dark gray claystone upwards.

Member C consists of phosphatic limestone, bioturbated limestone, marl, and claystone. It was also divided into three units (6, 7, and 8). Unit-6 begins with phosphatic limestone, continues with the bioturbated limestone, and grades into limestone. Unit-7 and unit-8 consists of marl and claystone, which were not studied here.

Eighty-three samples were taken from Member A, Member B, and the lower part of the Member C (between 139.87 and 74.45m). Sixty-six of these samples were taken from Member A, twelve samples from Member B, and the last five samples were taken from the lower part of Member C. In general, the sampling interval was 1 m but it was increased to 30 to 50 cm where necessary, such as between 111.0 and 112.0 meters. The resolution was highest (1 to 3 cm) between 80.00 and 79.00 meters in order to delineate precisely the location of the K/Pg boundary.

2.2.2 Methods

2.2.2.A Sample Preparation

Because of their high clay content and strong induration, the lithologies recovered from the core were not amenable to disaggregation in water, and the standard methods of preparation used in foraminiferal studies were unsuccessful for isolating foraminifera for taxonomic analysis. In addition, several attempts at using separately preparing methods involving acidic or basic treatments of the rocks (Lirer, 2000; McNeil et al., 2000;

Karimina, 2004, i.e.) did not result in sufficient recovery of microfossils. Thus a new methodology (Consecutive uses of dilute acidic and basic solution; DAB) was devised for this study. It consists in the consecutive use of dilute acidic and basic solutions to extract foraminifera from the rocks (see Chapter 1 of this thesis). Depending on the lithology, 80% and 90% dilute acetic acid and 8.25% sodium hypochlorite containing regular bleach was used for the extraction. Slow heating and/or rapid boiling of these solutions were complementary applications based on the lithology and decrease the processing time. 5-21 grams of sediment were used for the extraction depending on the amount of sample available, and considering that splits of the original samples were kept for optional subsequent studies. DAB allowed the recovery of sufficient amounts of residues >125 μm for the micropaleontological study conducted here. Even though the overall recovery was less than 1 g per sample, foraminifera were abundant (>300 specimens per sample) and diverse. After DAB, the quality of preservation was good to excellent except at some levels, where it was poor to moderate due to overexposure.

Following the DAB treatment, the residue obtained from each sample was split using a microsplitter. One half of the split residue was stored for archival purposes, whereas the other half was sieved through 250 μm, 150 μm and 125 μm sieves for qualitative and quantitative analysis. A Zeiss STEM 200 stereomicroscope was used for taxonomic determination. Light microscope and scanning electron microscope (SEM) images of selected specimens were taken to illustrate the diversity and remarkable preservation of the planktonic foraminifera encountered in the Upper Cretaceous and lower Paleocene of the core (plates 2.1 and 2.2).

All specimens encountered in each split of the residues from the washed samples were picked and determined at species level. This provided a basis for documentation of the foraminiferal diversity. This procedure was different from the general practice, which consists in picking, identifying, and counting only 300 specimens encountered in washed residues. Only occasionally less than 300 specimens were recovered from a split residue and no additional sample was prepared (table 2.2). After taxonomic identifications, specimens were mounted on labeled cardboard slides for archival purposes and counting. The number of foraminifera per gram was computed, using the dry weight of the initial sample, the number of foraminifera counted and the split fraction. In addition, the relative abundances of each genus were given in percentage per sample (appendix 2.1).

The < 125µm fraction was not studied because juvenile forms are not easily identified at the species level. Pyritization hampered proper identifications of taxa in unit 1 except at 137.50 meter. The sample from this level was only used for biostratigraphic interpretation.

A 1.68 m thick claystone interval was present between 79.50 and 77.82 meters. This interval was of major importance in delineating the base of the *Guembelitria cretacea* PRZ (P0) in the succession. Three samples from this interval were processed twice; however, none of these attempts resulted in the recovery of planktonic foraminifera. As a last resort, this claystone interval was examined without applying any washing technique. Samples were crushed, and directly analyzed under the stereomicroscope. No planktonic

foraminifera were found and the matrix of the rock was illustrated with stereomicroscopic images (fig. 2.3).

2.2.2.B Biozonal framework

This study relies on three biozonal frameworks. For the Maastrichtian Stage, I used the biozonal framework of Caron (1985) in combination with the biozonal framework of Li and Keller (1998a, b) established for the upper part of the Maastrichtian Stage (fig. 2.4). For the Danian Stage, I used the biozonal framework of Wade et al. (2011). A comparison of biozonal frameworks shows the zonal markers for the Maastrichtian and Danian (fig. 2.5).

2.2.2.B.1 *Maastrichtian Biostratigraphy*

The globotruncanid-based standard biozonal framework of Caron (1985) is one of the most widely accepted for the Tethyan Realm. Caron (1985) divided the Maastrichtian Stage into four biozones, which are, in stratigraphic sequence: the *Globotruncana havanensis*, *Globotruncana aegyptiaca*, *Gansserina gansseri,* and *Abathomphalus mayaroensis* zones. The lowest zone was not encountered in this study. The *Globotruncana aegyptiaca* Zone is defined as the interval between the lowest occurrence (LO) of *Globotruncana aegyptiaca*, and that of *Gansserina gansseri*. The *Gansserina gansseri* Zone is the interval between the LO of *Gansserina gansseri* and the LO of *Abathomphalus mayaroensis*; and the *Abathomphalus mayaroensis* Zone is defined by the total range of the nominate taxon. The top of the zone corresponds to the top of the Maastrichtian. Although Caron's biozonation is widely used, it has also several important

shortcomings. The scarcity or absence and the diachronous occurrences of globotruncanids tend to obstruct the application of this biozonal framework in shallow water stratigraphies (Li and Keller, 1998 a, b). More importantly, no specimens of *A. mayaroensis* were recovered in the DQC core. This is due to the fact that *A. mayaroensis* is a deep water taxon, so that the youngest Maastrichtian zone (the *A. mayaroensis* Zone) cannot be identified in shallow water (neritic) stratigraphies,

For such shallow-water successions, thermophilic heterohelicids and some other tropical-subtropical globigerinids such as *Plummerita hantkeninoides* have proven useful for correlation (Arenillas et al., 2004; 2006), and a relatively more reliable biozonation has been established by Li and Keller (1998a) based on these taxa. A point in case here is that the relative abundances of globotruncanids did not exceed 27.1% at any level in the DQC, whereas the genera of the family *Heterohelicidae* were diverse and abundant, with percentages varying between 42.8% and 90.9% in the upper Cretaceous strata (Appendix 2.1).

Li and Keller (1998 a, b) substituted four heterohelicid zones for the upper part of the *G. gansseri* and *A. mayaroensis* zones of Caron (1985) as shown in figure 2.4. In stratigraphic succession these are:

The Racemiguembelina fructicosa **Partial Range Zone (PRZ) (Li and Keller, 1998a):** Interval between the LO of *Racemiguembelina fructicosa* and the LO of *Abathomphalus*

mayaroensis. Li and Keller (1998a) showed that the base of this zone corresponds to the upper part of the *G. gansseri* Zone of Caron (1985).

***The Pseudoguembelina hariaensis* Partial Range Zone (PRZ) (Li and Keller, 1998a):** Partial range of the nominate taxon from its LO to the highest occurrence (HO) of *Gansserina gansseri*.

***The Pseudoguembelina palpebra* Partial Range Zone (PRZ) (Li and Keller, 1998a):** Partial range of the nominate taxon between the HO of *G. gansseri* and the LO of *P. hantkeninoides*.

***The Plummerita hantkeninoides* Zone Total Range Zone (TRZ) (Pardo et al, 1996):** The total range of *Plummerita hantkeninoides* indicating the uppermost Maastrichtian Stage.

All these marker species were recovered from the DQC samples.

2.2.2.B.2 *Danian Biostratigraphy*

P0: *Guembelitria cretacea* Partial Range Zone (PRZ) (Wade et al., 2011): Partial range of *Guembelitria cretacea* between the HO of Cretaceous genera (globotruncanids, rugoglobigerinids, etc.), and the LO of *Parvularugoglobigerina eugubina*, which is the index marker of Zone Pα.

Remarks: Zone P0 is the lowermost biozone of the Cenozoic (Olsson et al., 1999; Wade et al., 2011).

Pα: *Parvularugoglobigerina eugubina* Total Range Zone (TRZ) (Wade et al., 2011): Total range of the nominate taxon *Parvularugoglobigerina eugubina*.

Remarks: Olsson et al. (1999) reported several species with LOs in Zone P0, and continuing into Zone Pα. These are *Guembelitria cretacea*, *Rectoguembelina cretacea*, *Zeauvigerina waiparaensis*, *Parvularugoglobigerina alabamensis*, *Prv. extensa*, *Globanomalina archaeocompressa*, *Eoglobigerina eobulloides*, *Praemurica taurica*, and *Parasubbotina* aff. *pseudobulloides* in the order of stratigraphic appearances.

2.2.2.C Biochronology

This study follows the biochronology in Gradstein et al. (2012) for the Maastrichtian and Danian interval. This allows a resolution of 0.1 to 1.5 Myr between datums (table 2.1).

Gradstein et al. (2012) reported uncertainties associated with some of the Maastrichtian biostratigraphic events. Latitudinal diachrony was reported for the first appearance datum (FAD) of *Racemiguembelina fructicosa*. Multiple ages were given for the FADs of *Planoglobulina acervulinoides*, and *Pseudotextularia elegans*. The FAD of *P. acervulinoides* was located by Gradstein et al. (2012) in late Campanian, where it is simultaneous with the FAD of *Gansserina gansseri* at 72.97 Ma. It was also placed by these authors at 70.05 Ma in the Maastrichtian. This large uncertainty (>2.5 Myr) may be due to ambiguous taxonomic concepts (Gradstein et al., 2012). Similarly, the FAD of *P. elegans* was given at the same level as the LAD of *Radotruncana calcarata*, at 75.71 Ma (Campanian), but also at 69.55 Ma, in the Maastrichtian. The lifespan of *P. hantkeninoides* was estimated to correspond approximately to the last 350 kyr of the Maastrichtian (Gradstein et al., 2012).

Some other Maastrichtian datum levels such as the FAD of *Contusotruncana contusa* (71.01 Ma), the LAD of *Globotruncana ventricosa* (70.14 Ma), and the LAD *Rugoglobigerina pennyi* (68.86 Ma) were not applicable because of inconsistent stratigraphic occurrences in the DQC. Additionally, *Abathomphalus mayaroensis* (see above) and *Contusotruncana patelliformis* were not recorded in the succession.

2.2.2.D Sedimentation Rate (SR) curve

Sedimentation rate (SR) curves are used to determine the completeness of stratigraphic sections. Aubry (1995) extensively discussed the importance of differentiating between stratigraphic occurrences such as LOs and HOs and temporal events such as FAD and LAD. On this basis, she emphasized the importance of sound temporal interpretations of stratigraphic successions and the significance of unconformities. The best temporal interpretations of sections are derived from the use of multiple stratigraphic means, including magnetochronology and biostratigraphy (see Aubry, 1995 for detailed explanations). However, in this study no independent calibration tool such as magnetochronology was available. Therefore, confident delineation of unconformities and hiatuses increase with the numbers of stratigraphic datums used to constrain sedimentation rate curves. In this study two sets of data are available to construct sedimentation rate curves for the Maastrichtian interval studied here: the planktonic foraminiferal datum levels and the calcareous nannofossil datum levels as delineated by Aubry and Salem (2012a). These datums were plotted by stratigraphic position in the core against their age in Gradstein et al. (2012) (table 2.1 and 2.3).

I refrained from attempting to construct a sedimentation rate curve for the Paleocene for three reasons. First, the number of planktonic foraminiferal biohorizons recognized in this study wasnot sufficient for a high-resolution interpretation. Second, Obaidalla (2012) showed a hiatus spanning the *P. hantkeninoides* TRZ and *G. cretacea* PRZ (P0), most likely due to the low sampling resolution in his study. Third, I show here the presence of the base of Zone Pα at 75.72 m marked by the LO of *Prv. eugubina*. However, this LO was reported by Obaidalla (2012) at 80.20 m in DQC (see discussion below). Fourth, Aubry and Salem (2012a) already conducted a temporal interpretation of the Paleocene and lower Eocene succession in the DQC, combining planktonic foraminifera and nannoplankton datum levels. Their results were used as complementary in this study.

2.2.2.E Relative abundance plots

Relative abundance plots were prepared to determine the stratigraphic patterns of planktonic foraminifera at the family and generic levels. The data upon which the abundance patterns are established are tabulated in Table 2.2 and Appendix 2.1.

The procedure followed here consisted in cross-plotting the abundances of *Heterohelicidae*, *Globotruncanidae*, and *Rugoglobigerinidae,* three families that contain the most widely used biostratigraphic markers for the Upper Cretaceous (figure 2.6 and 2.7). The reason for adding rugoglobigerinids was that some of their species have also been used for biostratigraphic purposes (Arenillas et al., 2004; 2006). Rugoglobigerinids, globotruncanids, and heterohelicids live primarily in the mixed layer (Abramovich et al., 2003).

2.3 Results

The results of this study are to 1) provide a biozonal subdivision of the stratigraphic succession recovered from the Dababiya core between 140.0 and 74.45 m; 2) determine its chronostratigraphic age and to locate the Cretaceous/Paleogene boundary; 3) evaluate the completeness of the succession through the construction of a sedimentation rate curve; and 4) illustrate the abundance patterns of biostratigraphically important planktonic foraminifera at different taxonomic levels in the DQC.

2.3.1. Biozonal assigment

In this study, the *Gansserina gansseri* Zone of Caron (1985) was recognized and subdivided into the *G. gansseri* LOZ (lower part), and *R. fructicosa* LOZ (upper part). The *A. mayaroensis* biozone of Caron (1985) was not identified but the correlative heterohelicid-based zones of Li and Keller (1998a) were substituted. These are the *Pseudoguembelina hariaensis* PRZ; *Pseudoguembelina palpebra* PRZ; *Plummerita hantkeninoides* TRZ biozones. Figure 2.8 shows all the taxa present in the biozonal succession.

The *Globotruncana aegyptiaca* LOZ constitutes the lowest 2.50 meters of the core (between 140.0 and 137.50 m). *Globotruncana aegyptiaca* was represented by a few specimens only with moderate to good preservation. The lithology in this zone is claystone (fig. 2.2), and pyritization prevented firm taxonomic identifications at some level, such as at 139.87 m.

The interval between 137.50 and 110.50 m is assigned to the *Gansserina gansseri* LOZ between the LO of *Gansserina gansseri* at 137.50 m and the LO of *Racemiguembelina fructicosa* at 110.50 m. Only one specimen of *Gansserina gansseri* was recovered at 137.50 m, where the LO of the species is placed. This index taxon occurs consistently above 134.50 meter in DQC and up to 84.55 m, where its HO is placed. From 134.50 m upsection, the index marker is relatively abundant and its preservation was moderate to good for a proper identification (figure 4 and 5; plate 2.1).

The *Racemiguembelina fructicosa* LOZ is placed between 110.50 m (the LO of *R. fructicosa*) and 91.50 m (the LO of *P. hariaensis*) in the core. Only one specimen of *R. fructicosa* was recovered from level 110.5 m. Above this, the marker is sporadically present and its abundance never exceeded 5 specimens. This index species exhibits distinctive sieve-plate and bridge-like morphological features (see Nederbragt, 1991 for details). The test recovered at 110.5 m was partially broken; however, complementary morphologic features were sufficient for a confident identification.

In the DQC, the *Pseudoguembelina hariaensis* PRZ extends from the LO of *P. hariaensis* at 91.50 to the HO of *G. gansseri* at 84.55 meters. *Pseudoguembelina hariaensis* was present (only a few specimens) at two levels in the core, one level being its LO at 91.50 m and the other at 84.55 m, a level that also corresponds to the HO of *G. gansseri*. The preservation of the index markers was good and identification is confident (figure 7 and 8; plate 2.1).

The *Pseudoguembelina palpebra* PRZ was delineated between the HO of *G. gansseri* (84.55 m) and LO of *P. hantkeninoides* (82.50 m) in the core.

The uppermost Maastrichtian *Plummerita hantkeninoides* TRZ was defined between the LO (82.50 m) and HO of *P. hantkeninoides* (81.05 m). The index taxon was abundant and well preserved, which ensured its proper taxonomic identification (figure 9 and 10; plate 2.1).

Guembelitria cretacea PRZ (P0) was defined as the partial range of *G. cretacea* between the HO of Cretaceous characteristic genera (*Archaeoglobigerina*, *Globotruncana*, *Globotruncanella*, *Globotruncanita*, *Rugoglobigerina*, *Rugotruncana,* etc.) and the LO of *Prv. eugubina*, the marker of Zone Pα.

The oldest Danian planktonic foraminiferal assemblage in this study were found at 77.70 meter. They contain the HOs of the K/Pg boundary survivor taxa *Guembelitria cretacea*, *Hedbergella holmdelensis*, and *Hedbergella monmouthensis* and the LOs of the lower Danian genera. One specimen of the index taxon *G. cretacea* was found at this level (77.70 m). It displayed the distinctive triserial morphology that permitted a firm identification (figure 1 and 2; plate 2). Hedbergellids were abundant with approximately 60 specimens among the survivor taxa. The preservation of hedbergellids was moderate (figure 3-5; plate 2).

Olsson et al. (1999) reported the FADs of *Parvularugoglobigerina extensa*, *Globanomalina archaeocompressa*, *Eoglobigerina eobulloides*, *Praemurica taurica*, *Parasubbotina* aff. *pseudobulloides* (in order of first appearances) within Zone P0. The simultaneous LOs of *Eoglobigerina* (*E. eobulloides*, *E. edita*, *E. praedita*,), *Globanomalina* (*G. archaeocompressa*), and *Parasubbotina* (*P.* aff. *pseudobulloides*),together with the HOs of the survivor taxa *Hedbergella holmdelensis*, *H. monmouthensis*, and *Guembelitria cretacea* is a result of the barren interval immediately below 77.70 m, not the indication of a hiatus in the core.

The *Parvularugoglobigerina eugubina* TRZ Pα is defined as the total range of the index species. In this study he LO of the zonal biomarker *Prv. eugubina* was recorded at 75.72 m in the core. This species was not present in great abundance at this level. Its HO is higher than the youngest stratigraphic level studied here, which is 74.45 m.

2.3.2 Sedimentation rate (SR)

Table 2.1 shows the planktonic foraminiferal and nannoplankton biohorizons used in the temporal interpretation of the succession. In the DQC, the planktonic foraminiferal biohorizons showed a reasonably good alignment (fig. 2.9) except at one interval between the HO of *G. gansseri* and the pyritized fossil layer (PFL, used as a proxy for the K/Pg boundary).

2.3.3 Relative abundance patterns

In the DQC, heterohelicids were almost twice as abundant as globotruncanids and rugoglobigerinids at almost all levels (fig. 2.6). Three stratigraphically close levels are marked by a remarkable dominance by one family (fig. 2.6): *Heterohelicidae* at level 128.10 m; *Rugoglobigerinidae* at 123.50 m, and *Globotruncanidae* at 118.67 m. The abundance patterns of the three families change in the core. The *Heterohelicidae* increase in abundance upwards associated with high generic and species diversity. In contrast, the rugoglobigerinids decrease in abundance upsection, and the globotruncanids are mostly abundant in the mid-part of the core between 123.0 m and 91.0 m. Three stratigraphic intervals are of particular interest.

At 128.10 m (yellow line), abundance of these taxa are (fig. 2.6): heterohelicids*:* 74.8%, globotruncanids: 7.2%, and rugoglobigerinids: 7.9%. At 118.67-.65 m (blue line), the abundance of the same taxa are heterohelicids*:* 58.1%, globotruncanids: 25.8% for and rugoglobigerinids: 13.3%. At 123.50m (red line), the relative abundances are heterohelicids: 48.8%, globotruncanids: 7.4%, and rugoglobigerinids: 40.9%.

Six stratigraphic levels are marked by an enrichment in one of the three selected genera together with concurrent changes in abundance of the other two taxa (fig. 2.7).

The *Heterohelix* spp. peak (61.8 %) at 133.27 m is accompanied by low abundance of *Pseudoguembelina* spp. (14.5%), and *Pseudotextularia* spp. (8.2%). The highest peak in *Pseudoguembelina* spp. at 121.25 m also corresponds to a decrease in abundances of *Heterohelix* spp. (13.8%), *Pseudoguembelina* spp. (43.7%) and *Pseudotextularia* spp.,

(19.5%). An abundance peak in *Pseudotextularia* spp. (51.2%) at 111.91 meter correlates with low abundances of *Heterohelix* spp. (8.3%) and of *Pseudoguembelina* spp. (13.9%). This level is marked by the lowest abundance of *Heterohelix* spp. in the succession.

Another peak in abundance (41.3%) of *Heterohelix* spp. occurs at 109.22 m marked by low abundance of *Pseudoguembelina* spp. (15.2%), and of *Pseudotextularia* spp. (20.6%).

Pseudoguembelina spp. peaks in abundance (29.8%) at 95.50 m, where the abundances of *Heterohelix* spp. and *Pseudotextularia* spp. are equal (19.2%).

The youngest remarkable stratigraphic level is at 87.47 m, where *Heterohelix* spp. has a marked peak in abundance (51.5%,) At this level, abundances of *Pseudoguembelina* spp. and *Pseudotextularia* spp. are 21.2% and 3.0%. This is the lowest abundance level of *Pseudotextularia* spp. in the core.

2.4 Discussion and Conclusions

The data presented here complement previous studies of the Dababiya Quarry core in 1) establishing a biozonal framework for its Cretaceous interval; 2) refining the age of the oldest Danian deposits, and 3) showing that the Maastrichtian interval recovered from the core is temporally almost continuous. In addition, this study suggests a potential for use of the abundance peaks of heterohelicids for biostratigraphic purposes.

2.4.1 Biozonal age of the DQC (140.0 and 74.45 m)

2.4.1.A Upper Cretaceous

This study combined the biozonal schemes of Caron (1985) and Li and Keller (1998a) in order to provide a higher resolution for interpretations. I assign the bottom of the core (between 140.0 and 137.50 m) to the *G. aegyptiaca* LOZ. Aubry and Salem (2012a) reported that the biozonal age of the base of the core was uncertain due to poor preservation of the calcareous nannofossils.

Obaidalla (2012) determined that the uppermost Maastrichtian *P. hantkeninoides* TRZ is absent. In contrast, this study shows the occurrence of *P. hantkeninoides* in the core and I assign the interval between 82.50 and 81.05 m to the *P. hantkeninoides* TRZ.

2.4.1.B Lower Danian

This study adopted the planktonic foraminiferal biozonation of Wade et al. (2011). Lower Danian Zone P0 (*G. cretacea* PRZ) and Pα (*Prv. eugubina*) were identified, spanning the interval between 77.7 and 74.45 m with the P0/ Pα zonal boundary at 75.72 m. Based on the samples analyzed in this study the planktonic foraminifera are absent between 81.05 m (the HO of *P. hantkeninoides*) and 77.70 m LO (*G. cretacea*). This interval consists predominantly of non-carbonate, black claystone (Dupuis and Knox, 2012). The upper 1.68 m of this barren interval consists of claystone and was intensively studied in the hope of finding planktonic foraminifera to determine the base of the Zone P0, however none were found. Our data conflicts with Obaidalla (2012), who reported the occurrence of *Prv. eugubina* at level 80.0-80.02 m, a record that we cannot confirm. However, the

specimens illustrated by this author are characteristic. Possible explanations for the discrepant record of *Prv. eugubina* are: 1) use of different sets of samples; 2) downhole contamination in the core; 3) delayed LO of *Prv. eugubina* due to poor preservation and scarcity below 75.72 m. The interval between the LO of *Prv. eugubina* and the PFL is assigned to Zone P0.

2.4.2 Chronostratigraphic age

Based on the planktonic foraminiferal zones identified here, the interval between 137.50 m and 74.45 m in the DQC is Maastrichtian to Danian in age. The interval between 137.50 and 81.05 isMaastrichtian. The age of the base of the core is uncertain. Based on Gradstein et al. (2012), the FAD of *G. gansseri* is at 72.97 Ma and that of *G. aegyptiaca* is at 74.00 Ma. Below 137.50 m, only *G. aegyptiaca* was recorded but species determination was tentative because most foraminiferal tests were pyritized, which hampered proper identifications. Preservation uncertainties raise two possibilities: *G. gansseri* may be present below 137.50 m in the form of a few pyritized specimens; alternatively, *G. gansseri* may be present only above 137.50 m in which case the basal 2.50 m of DQC belongs to the *G. aegyptiaca* Zone, where the nominate taxon was recovered. The K/Pg is not precisely characterized based on planktonic foraminifera (see above and below). Dupuis and Knox (2012) used a pyritized ammonite-rich layer at 80.36 m to approximate it. This is in agreement with placement of the boundary between 80.4 and 80.2 m in the core following the nannoplankton biostratigraphic results of Aubry and Salem (2012a).

2.4.3 Completeness of the section

One of the major applications of biostratigraphy is the estimation of stratigraphic continuity. As stated by Aubry (1995), even the thickest deep-sea sections may not be as complete as they initially appear. Here, I discuss the continuity of DQC succession based on the sedimentation rate (SR) results (fig. 2.9).

The Campanian(?) to Maastrichtian interval would appear to be temporally continuous between 135.5 and 82.98 m (fig. 2.9). Although the sedimentation rate curve is constrained by only planktonic foraminiferal biohorizons and a single calcareous nannofossil datum, these datum levels fall remarkably close to a straight lineThe only discrepant datum is the LO of *Planoglobulina acervulinoides* (at 101.50 m), whose age is poorly calibrated (see above).

This implies that the erosional surfaces described in the core by Dupuis and Knox (2012) are not associated with major hiatuses. This is particularly true for the surface at 82.98 m. We calculated an apparent sedimentation rate of about 1.23 cm/kyr for the Upper Cretaceous part of the core (Table 2.3).

There is a discrepancy at ~83.75 m between the planktonic foraminiferal datum (LO of *P. hantkeninoides* at 82.50 m with FAD at 66.39 Ma) and the calcareous nannoplankton biohorizons: 1) the LO of *Micula murus* at 83.9 m with a FAD at 69.00 Ma; 2) the LO of *Nephrolithus frequens* at 83.0 m with an age of 67.84 Ma. Inasmuch as the HO of *Micula prinsii* falls on the line of correlation. We question the reliability of the LOs of *M. murus*

and *N. frequens* as delineated by Aubry and Salem (2012a). These authors recognized that the LO of *N. frequens* may have been problematic because this species is generally rare at low latitudes.

The sedimentation rate curve for the lower Danian part of the core studied here is poorly constrained (2.10). First, there is a problem with the location of the LO of *Prv. eugubina* (see above). Second, the interval between 79.70 and 77.70 consists of dark brown clay and is barren of planktonic foraminifera (although there are scarce fragments of benthic foraminifera). Our placement of the LO of *Prv. eugubina* at 75.72 m would imply that Zone P0 is 4.64 m thick, which in turn, would imply a sedimentation rate of 116 cm/kyr. For this interval such an extremely high average rate of sedimentation is highly unlikely. In contrast, the placement of the LO of the *Prv. eugubina* at 80.0-80.02 m following Obaidalla (2012) implies that Zone P0 is only 20 cm thick, implying, in turn, a low sedimentation rate of 0.5 cm/kyr for this interval, which is more reasonable. We conclude from this that the K/Pg boundary in the core is essentially complete in the DQC. This conflicts with Obaidalla (2012) who inferred from the range of the planktonic foraminifera the presence of a stratigraphic gap in the section with a hiatus extending from at least the FAD of *P. hantkeninoides* to that of *Prv. eugubina*. We have shown here that *P. hantkeninoides* is present in this core. Its LO/FAD being located 2.14 m below the K/Pg boundary. If there is a hiatus in the vicinity of the K/Pg boundary, it has to be very short. On the other hand, the LO of *Cruciplacolithus tenuis* is located at 79.0 m at the same level as the HO of *Prv. eugubina* according to Obaidalla (2012). The FAD and

LAD of these two taxa are 65.47 Ma and 66.0 Ma, respectively. This may imply a short hiatus at about 77.82 m.

2.4.4 Abundance patterns

The patterns discussed here show strong correlations between the abundance of the biostratigraphically important planktonic foraminiferal families (*Heterohelicidae*, *Globotruncanidae*, and *Rugoglobigerinidae*) and between the genera of the family *Heterohelicidae*. Levels with high abundances of *Heterohelix* spp. are also levels with low abundances of pseudotextulariids and vice versa. The abundance of globotruncanids varies inversely with the abundance of heterohelicids (fig. 2.6).

The abundance patterns of *Heterohelix* spp. and *Pseudotextularia* spp. are inversely correlated throughout the Maastrichtian part of the core. These two genera dominated the planktonic foraminiferal assemblages except between 128.0 and 121.0 meter where *Pseudoguembelina* spp. are dominant. However, in the bulk of the section, *Pseudoguembelina* spp. occur generally in low abundances and in general, their abundances vary independently of those of *Heterohelix* spp. and *Pseudotextularia* spp.

Olsson et al. (2001) observed that the abundance of *Pseudotextularia elegans* was associated with the inputs of high-nutrient and oxygen-rich waters in the Atlantic during the Late Cretaceous. In contrast, *Heterohelicidae* abundances are associated with low-oxygen environments (personal comm. R. K. Olsson, 2014). Little is currently known about the ecology of the pseudoguembelinids. While high and low abundances of

Heterohelix spp. and *Pseudotextularia* spp. show strong correlations in the DQC (lines 1,3,4 and 6 in fig. 2.7), peak values of pseudoguembelinids do not exhibit such a relationship. This suggests that pseudoguembelinids are dependent on other ecologic thresholds than those that control the abundances of *Heterohelix* spp., and *Pseudotextularia* spp. In Gradstein et al. (2012), *Pseudoguembelina* spp. are regarded as reliable chronological markers. However, the abundance patterns in the DQC suggest that their occurrences may be determined by unknown ecological factors.

2.5 Epilogue

The Dababiya Quarry Corehole (DQC) has proven to contain an interesting Upper Cretaceous (Maastrichtian) section. Integration of biozonal schemes for ocean and epicontinental areas has permitted the establishment of a sedimentation rate curve, which indicates that the section is essentially continuous. Also sharp variation in abundance patterns of planktonic foraminifera characterize different parts of the section.

At this time the section has not been correlated with other sections from Egypt or adjacent basins but may eventually serve as a reference section for North Africa and the Middle East.

2.6 Acknowledgements

The author gratefully acknowledges his thesis advisors ProfessorsMarie-Pierre Aubry, Richard K. Olsson, and William A. Berggren for their guidance, patience, and generosity in sharing the experiences, as well as *Türkiye Petrolleri Anonim Ortakligi* (TPAO; Turkish Petroleum Corporation) for sponsoring and supporting this study.

2.7 References

Abramovich, S., Keller, G., Stüben, D., Berner, Z.. 2003. Characterization of late Campanian and Maastrichtian planktonic foraminiferal depth habitats and vital activities based on stable isotopes. Paleogeography, Paleoclimatology, Paleoecology 202, 1-29.

Alegret, L., and Ortiz, S., 2012. Uppermost Cretaceous to lowermost Eocene benthic foraminifera of the Dababiya Corehole, Upper Nile Valley, Egypt. Stratigraphy, vol. 9, nos 3-4, plates 1-2, table 1, pp. 267-277.

Arenillas, I., Arz, J.E., Molina, E., 2004. A new high-resolution planktic foraminiferal zonation and subzonation for the lower Danian. *Lethaia*, Vol. 37, pp. 79-95.

Arenillas, I., Arz, J.A., Grajales-Nishimura, J.M., Murillo-Muñetón, Alvarez, W., Camargo-Zanoguera, A., Molina, E., Rosales-Domínguez, C., 2006. Chicxulub impact event is Cretaceous/Paleogene boundary in age: New micropaleontological evidence. Earth and Planetary Science Letters. 249 (2006); 241-257.

Aubry, M.-P., 1995. From chronology to stratigraphy: Interpreting the stratigraphic record. In Berggren, W. A., Kent, D. V., Aubry, M.-P., and Hardenbol, J. (eds), Geochronology, Time scales and Global Stratigraphic Correlations: A Unified

Temporal Framework for an Historical Geology. Society of Economic Geologists and Mineralogists Special Volume No. 54, p. 213-274.

Aubry, M.-P., Ouda, K., Dupuis, C., Berggren, W. A., Van Couvering, J. A., and the Members of the Working Group on the Paleocene/Eocene Boundary, 2007. Global Standard Strato-type Section and Point (GSSP) for the base of the Eocene Series in the Dababiya Section (Egypt). Episodes, 30 (4), 271-286.

Aubry, M-P., and Salem, R., 2012a. The Dababiya Quarry Core: Coccolith Biostratigraphy. Stratigraphy, vol. 9, nos 3-4, plates 1-4, text figures 1-3, tables 1-4, pp. 241-259.

Aubry, M-P., and Salem, R., 2012b. The Dababiya Core: A window into Paleocene to early Eocene depositional history in Egypt based on coccolith stratigraphy. Stratigraphy, vol. 9, nos 3-4, plates 1-4, text figures 1-17, tables 1-5, pp. 287-346.

Berggren, W.A., Alegret, L., Aubry, M-P., Cramer, B.S., Dupuis, C., Goolaerts, S., Kent, D.V., King, C., Knox, R.W.O'B., Obaidalla, N., Ortiz, S., Ouda, K.A.K., Abdel-Sabour, A., Salem, R., Senosy, M.M., Soliman, M.F., & Soliman, A., 2012. The Dababiya Corehole, Upper Nile Valley, Egypt: Preliminary results. Austrian Journal of Earth Sciences, vol, 105/1, 161-168.

Caron, M., 1985. Cretaceous planktonic foraminifera. *In*: Plankton Stratigraphy. Bolli, H.M., Saunders, J.B., Perch-Nielsen, K. (eds), vol.1, 17-87.

Dupuis, C., and Knox, R.W.O'B., 2012. Lithostratigraphy of the upper Maastrichtian to lower Eocene succession in the Dababiya Corehole, Egypt. Stratigraphy, vol. 9, nos. 3- 4, pp. 205-212.

Gooalerts, S., and Dupuis, C., 2012. Ammonites from the Dababiya Corehole: Taxonomic notes and age assessment. Stratigraphy, vol. 9, nos 3-4, text-figures 1-2, table 1, pp. 261-266.

Gradstein, F.M, Ogg, J.G., Schmitz, M.D., et al., 2012, The Geologic Time Scale 2012: Boston, USA, Elsevier, DOI: 10.1016/B978-0-444-59425-9.00004-4.

Karimina, S.M., 2004. Extraction of calcified radiolaria and other calcified microfossils from micritic limestone utilizing acetic acid. Micropaleontology. Vol 50, no. 3, p 301-306.

Li, L., and Keller, G., 1998a. Maastrichtian climate, productivity and faunal turnovers in planktonic foraminifera in South Atlantic DSDP Sites 525A and 21. Marine Micropaleontology, 33, 55-86.

Li, L., and Keller, G., 1998b. Diversification and extinction in Campanian-Maastrichtian planktic foraminfera of northwestern Tunisia. Eclogae Geologicae Helvetica, vol. 91, p. 75-102.

Lirer, F., 2000. A new technique for retrieving calcareous microfossils from lithified lime deposits. Micropaleontology, v. 46, p. 365-369.

McNeil, D.H., Leckie, D.A., Kjarsgaard, B.A., Stasiuk, L.D., 2000. Agglutinated foraminiferal assemblages in Albian shales overlying kimberlite deposits in the Smeaton core from central Saskatchewan, Canada. *In*: Hart, M.B., Kaminski, M.A., & Smart, C.W., (eds). Proceedings of the Fifth International Workshop on Agglutinated Foraminifera. Gryzbowski Foundation Special Publication, 7 , 299-309.

Nederbragt, A. 1991. Late Cretaceous biostratigraphy and development of Heterohelicidae (planktonic foraminifera). Micropaleontology, vol. 37, no. 4, pp. 329-372, plates 1-12, text figs. 1-13, table 1.

Obaidalla, N., 2012. Planktonic foraminiferal biostratigraphy of the upper Cretaceous to mid-Paleocene of the Dababiya Quarry Corehole, Upper Nile Valley, Egypt. Stratigraphy, vol. 9, nos. 3-4, pp. 229-240.

Olsson, R.K., Hemleben, C., Berggren, W.A., Huber, B.A. (Eds), 1999. Atlas of Paleocene Planktonic Foraminifera: Smithsonian Contributions to Paleobiology, 85, 250 pages.

Olsson, R.K., Wright, J.D., Miller, K.G., 2001. Paleobiogeography of *Pseudotextularia elegans* during the latest Maastrichtian global warming event. Journal of Foraminiferal Research, v. 31, no. 3, p. 275-282.

Ouda, K., Berggren, W.A., Sabou, A.A., 2012. Planktonic foraminiferal biostratigraphy of the Paleocene/Eocene boundary interval in the Dababiya Quarry Corehole, Dababiya, Upper Nile Valley, Egypt. Stratigraphy, vol. 9, nos. 3-4, pp. 213-227.

Pardo, A., Ortiz, N., & Keller, G., 1996. Latest Maastrichtian foraminiferal turnover and its environmental implications in Agost, Spain. In: Cretaceous-Tertiary Mass Extinction: Biotic and Environmental Changes (Ed. by MACLEOD, N. & KELLER, G.), W.W. Norton & Co., New York, p. 139-172.

Wade, B.S., Pearson, P.N., Berggren, W.A., and Pälike, H., 2011. Review and revision of Cenozoic tropical planktonic foraminiferal biostratigraphy and calibration to the geomagnetic polarity and astronomical time scale: Earth Science Reviews, v.104, p. 111-142.

Youssef, M.M., 2003. Structural setting of central and south Egypt: an overview. Micropaleontology, vol. 49, supplement no. 1, pp.1-13, text-figures 1-6.

2.8 Figure Captions

Li and Keller (1998a,b) subdivided the Maastrichtian stage into two stages (lower and upper) and nine biozones (CF zones). These are CF9 *Globigerinelloides subcarinata*, CF8 *Globotruncana aegyptiaca*, CF7 *Gansserina gansseri*, CF6 *Rosita contusa*, CF5 *Pseudotextularia intermedia*, CF4 *Racemiguembelina fructicosa*, CF3 *Pseudoguembelina hariaensis*, CF2 *Pseudoguembelina palpebra* and CF1 *Plummerita hantkeninoides*, respectively.

Arenillas et al. (2004) also subdivided *Abathomphalus mayaroensis* and the upper part of the *Gansserina gansseri* biozones. In stratigraphically ascending order *Rugoglobigerina scotti*, *Planoglobulina acervulioides*, *Racemiguembelina fructicosa*, are consisting the upper part of the *Gansserina gansseri* zone and

Figures:

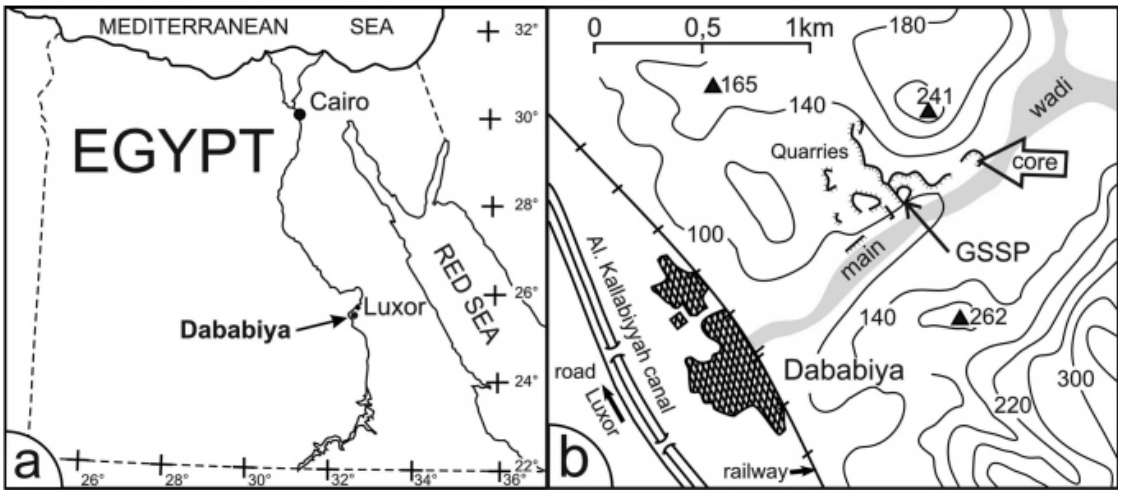

Figure 2.1

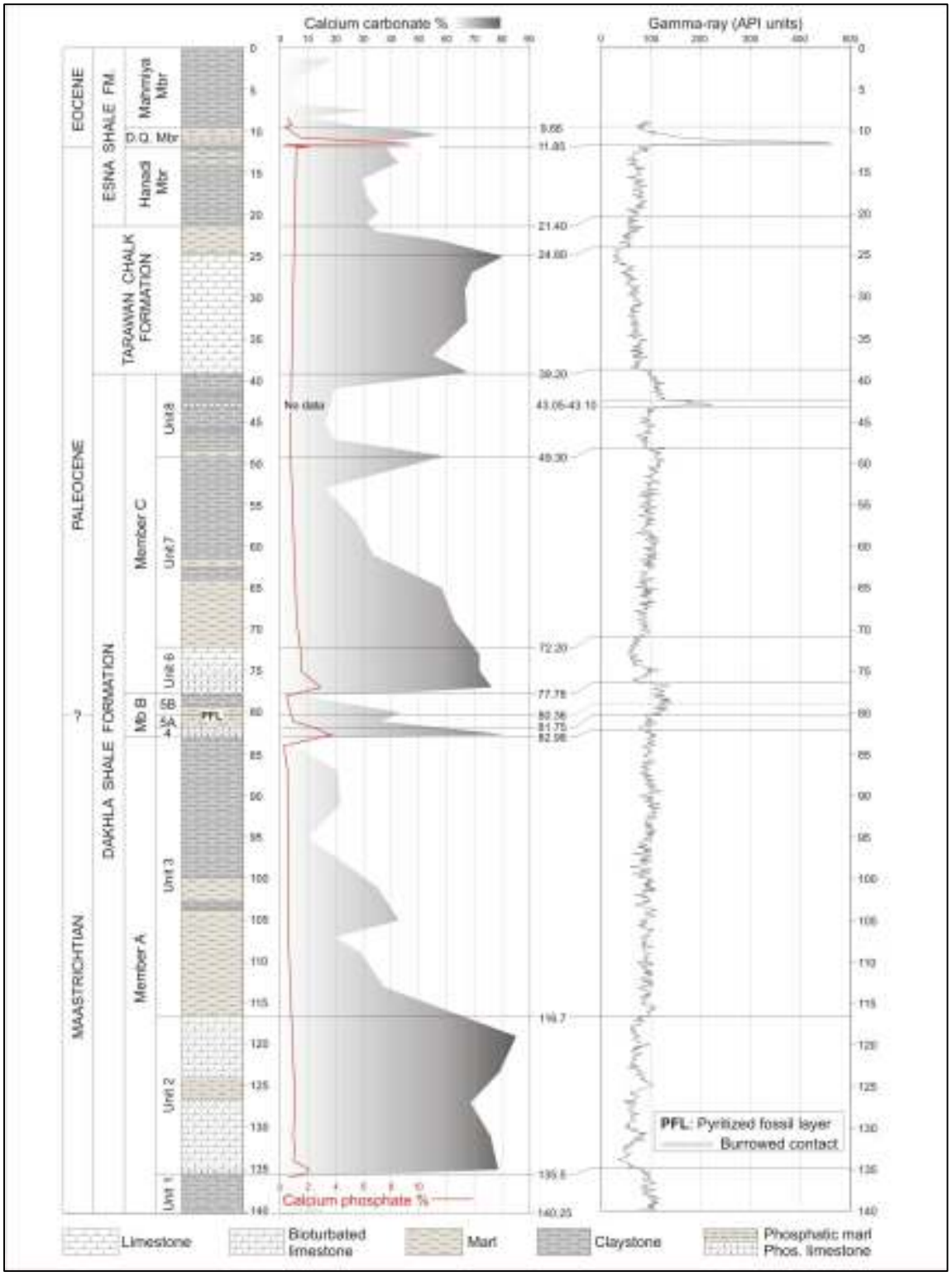
Calcium carbonate %
Gamma-ray (API units)
EOCENE
PALEOCENE
?
MAASTRICHTIAN
ESNA SHALE FM.
Mamniyat Mbr
D.D. Mbr
Hanadi Mbr
TARAWAN CHALK FORMATION
DAKHLA SHALE FORMATION
Member C
Member A
Mb B
Unit 8
Unit 7
Unit 6
Unit 3
Unit 2
Unit 1
PFL
No data
9.65
11.85
21.40
24.60
39.20
43.05-43.10
49.30
72.20
77.75
80.36
81.75
82.98
119.7
135.5
140.25
Calcium phosphate %
PFL: Pyritized fossil layer
Burrowed contact
Limestone
Bioturbated limestone
Marl
Claystone
Phosphatic marl
Phos. limestone

Figure 2.2

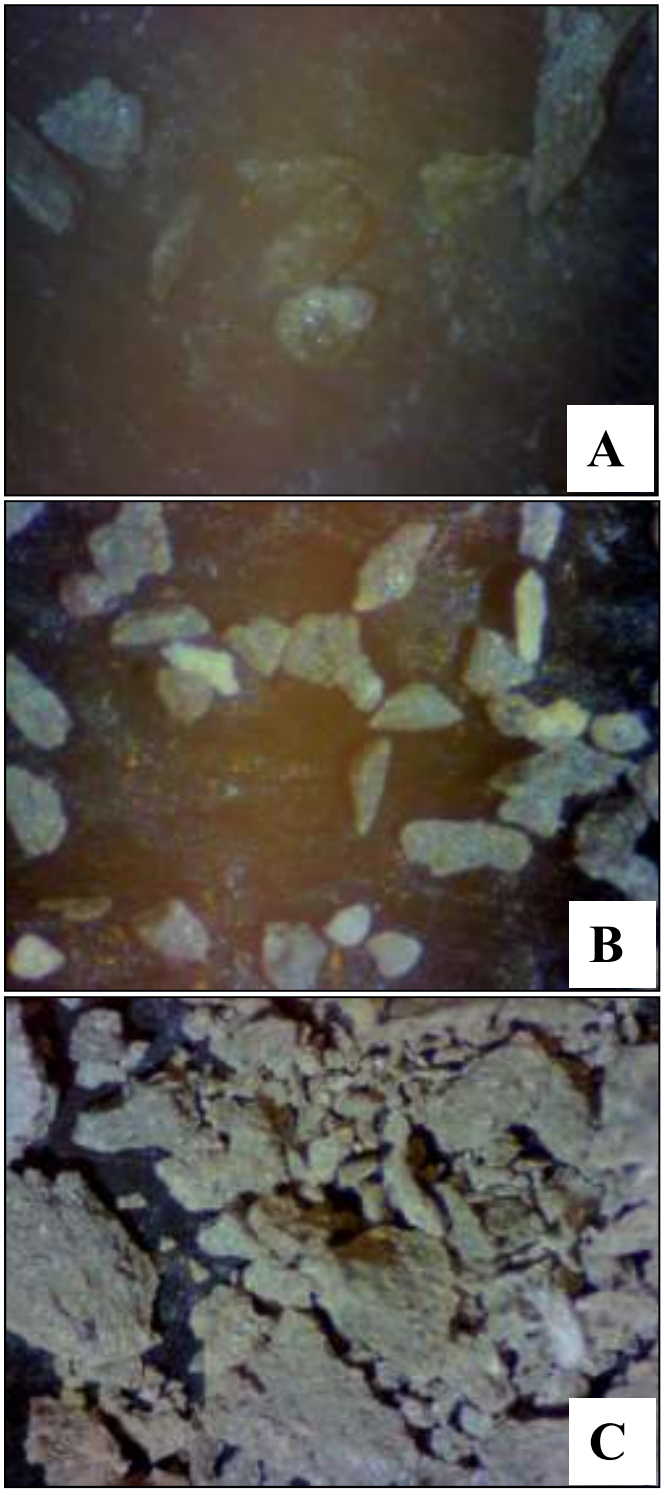

Figure 2.3

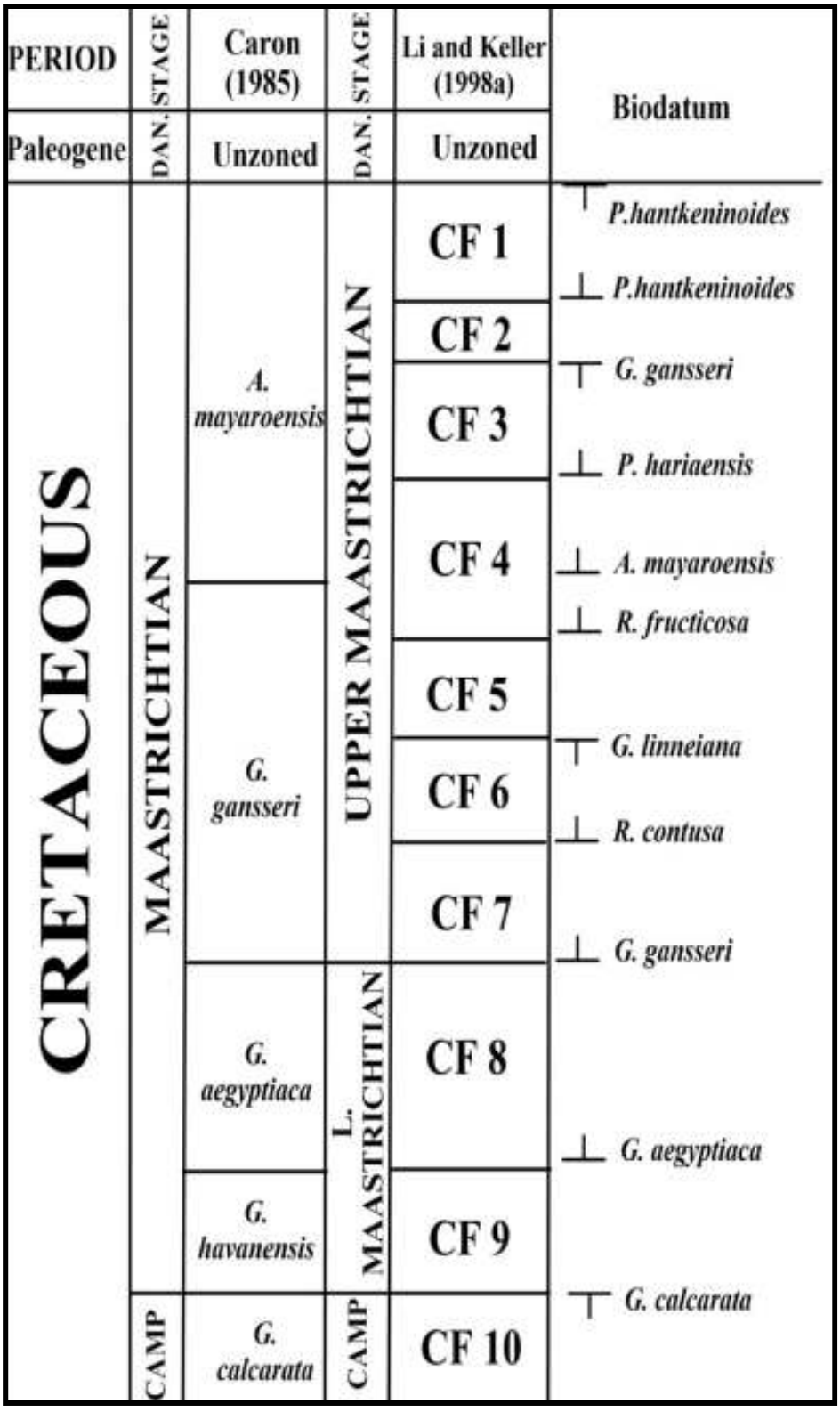
PERIOD
STAGE
Caron (1985)
STAGE
Li and Keller (1998a)
Biodatum
Paleogene
DAN.
Unzoned
DAN.
Unzoned
CRETACEOUS
MAASTRICHTIAN
UPPER MAASTRICHTIAN
L. MAASTRICHTIAN
A. mayaroensis
G. gansseri
G. aegyptiaca
G. havanensis
G. calcarata
CAMP
CAMP
CF 1
CF 2
CF 3
CF 4
CF 5
CF 6
CF 7
CF 8
CF 9
CF 10
P.hantkeninoides
P.hantkeninoides
G. gansseri
P. hariaensis
A. mayaroensis
R. fructicosa
G. linneiana
R. contusa
G. gansseri
G. aegyptiaca
G. calcarata

Figure 2.4

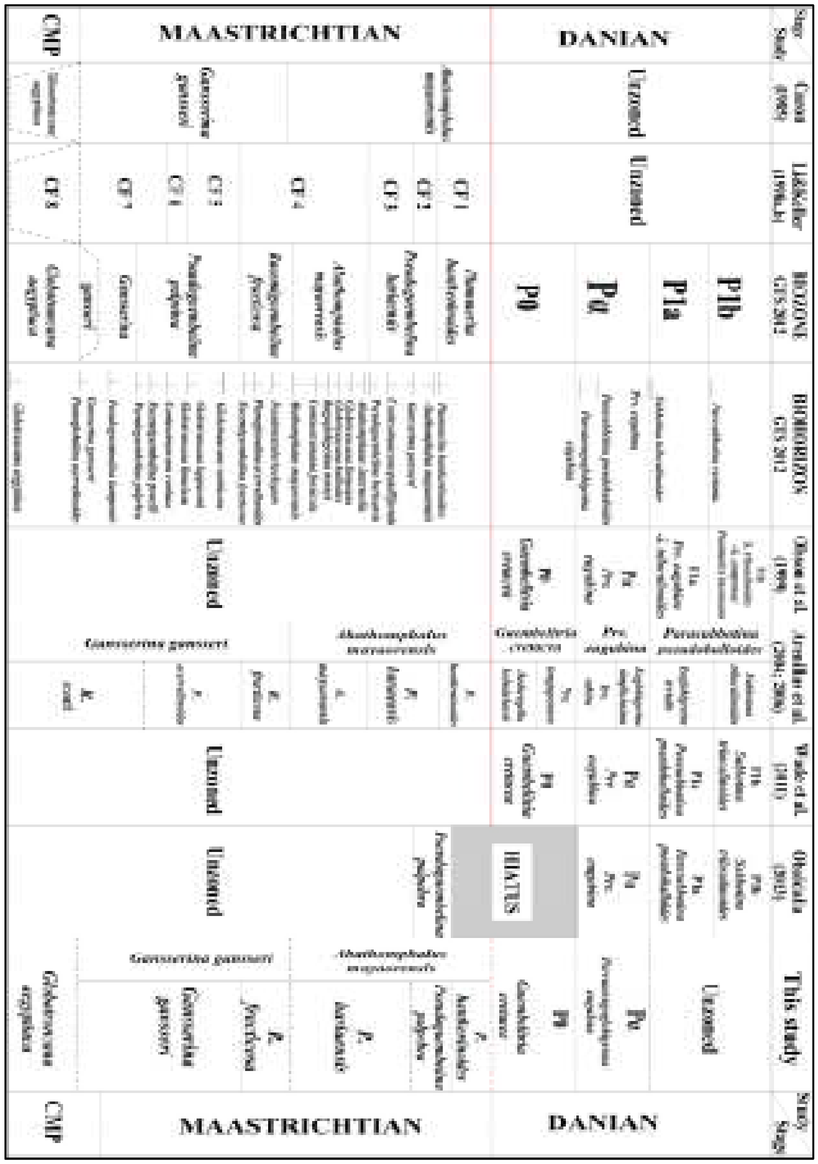

Figure 2.5

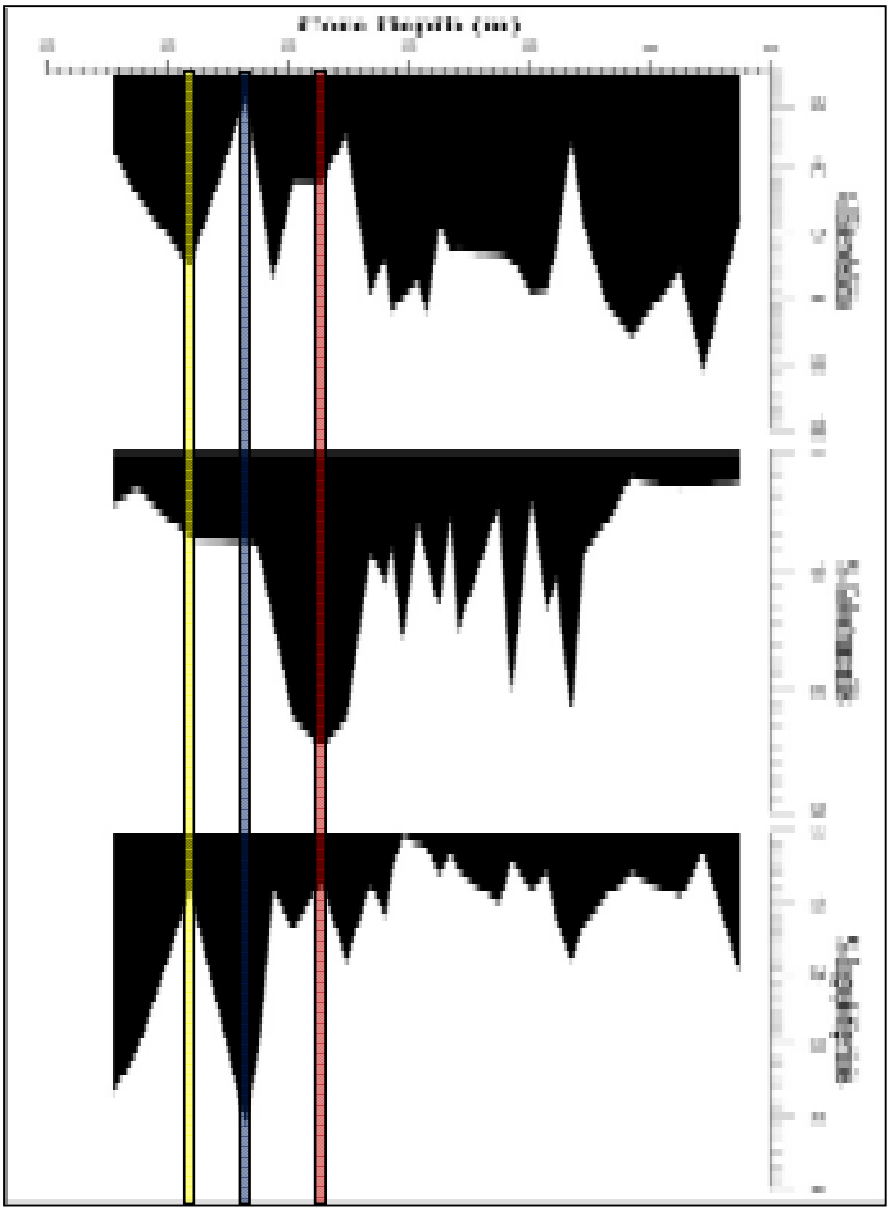

Figure 2.6

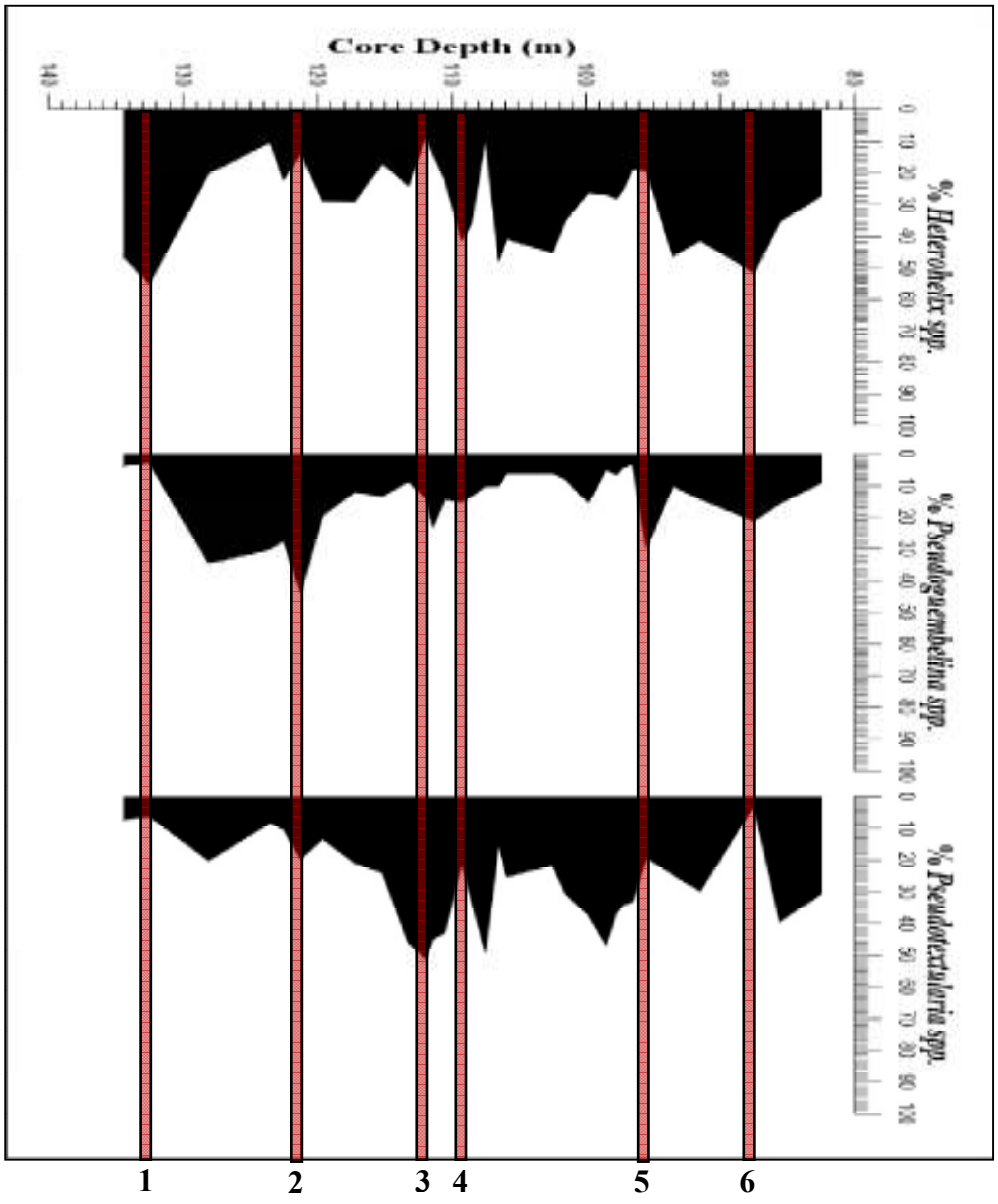
Core Depth (m)
% Heterohelix spp.
% Pseudoguembelina spp.
% Pseudotextularia spp.
1
2
3
4
5
6

Figure 2.7


Cretaceous
Paleogene
Period
Time Units
Maastrichtian
Danian
Age
Gansserina gansseri
R. fructicosa
P. acervulinoides
P. hariaensis
P. hantkeninoides
G. cretacea
P. eugubina
Biozone
Taxon
Archaeoglobigerina australis
Archaeoglobigerina blowi
Archaeoglobigerina mateola
Contusotruncana fornicata
Globigerinelloides prairihillensis
Globigerinelloides ultramicra
Globotruncana aegyptiaca
Globotruncana arca
Globotruncana mariei
Globotruncana cf. ventricosa
Globotruncanella petaloidea
Globigerinelloides subcarinatus
Globotruncanita conica
Globotruncanita stuarti
Globotruncanita falsostuarti
Globotruncanita stuartiformis
Heterohelix striata
Heterohelix sphenoides
Heterohelix carinata
Heterohelix globulosa
Heterohelix labellosa
Heterohelix moremani
Heterohelix navarroensis
Heterohelix cf. planata
Heterohelix rajagopalani?
Heterohelix punctulata
Heterohelix semicostata
Laeviheterohelix dentata
Laeviheterohelix glabrans
Planoglobulina cf. corsayae
Pseudoguembelina costellifera
Pseudoguembelina costulata
Pseudoguembelina excolata
Pseudoguembelina kempensis
Pseudotextularia elegans
Pseudotextularia intermedia
Pseudotextularia nuttali
Pseudotextularia deformis
Rugoglobigerina hexacamarata
Rugoglobigerina macrocephala
Rugoglobigerina milamensis
Rugoglobigerina reicheli
Rugoglobigerina rugosa
Rugoglobigerina scotti
Rugotruncana subpennyi
Rugotruncana subcircumnodifer
Gansserina gansseri
Pseudoguembelina palpebra
Racemiguembelina powelli
Globotruncana linneiana
Racemiguembelina fructicosa
Planoglobulina acervulinoides
Globotruncana bulloides
Pseudoguembelina hariaensis
Plummerita hantkeninoides
Guembelitria cretacea
Hedbergella holmdelensis
Hedbergella monmouthensis
Eoglobigerina eobulloides
Eoglobigerina edita
Eoglobigerina praedita
Eoglobigerina cf. simplicissima
Parasubbotina aff. pseudobulloides
Globanomalina archaeocompressa
Parvularugoglobigerina eugubina
Parvularugoglobigerina cf. sabina
Globanomalina planocompressa
Parasubbotina pseudobulloides
Praemurica taurica
Praemurica pseudoinconstans
Subbotina trivialis
Chiloguembelina morsei

Figure 2.8

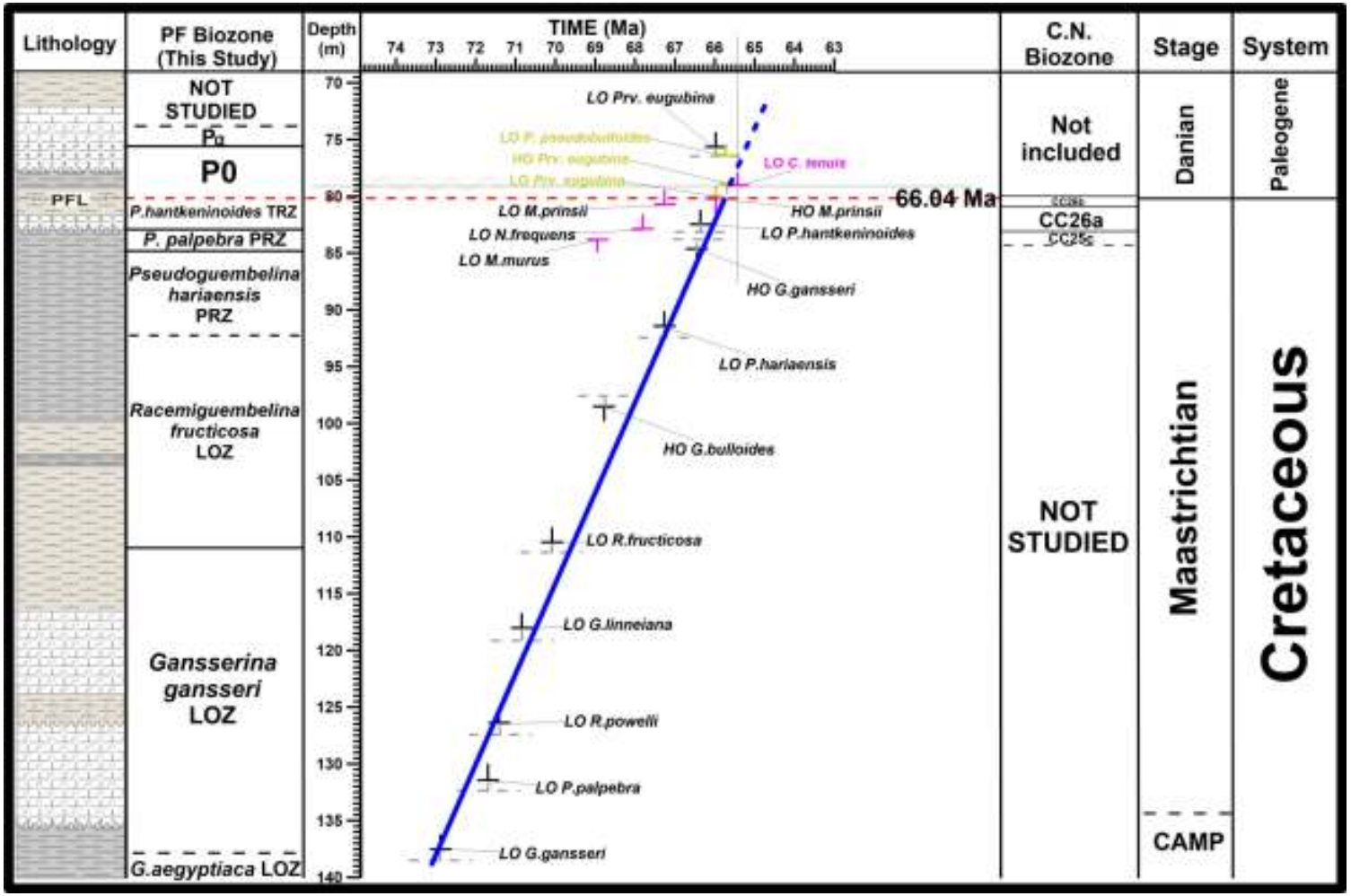
Lithology
PF Biozone (This Study)
Depth (m)
TIME (Ma)
74 73 72 71 70 69 68 67 66 65 64 63
C.N. Biozone
Stage
System
NOT STUDIED
Pα
P0
PFL
P.hantkeninoides TRZ
P. palpebra PRZ
Pseudoguembelina hariaensis PRZ
Racemiguembelina fructicosa LOZ
Gansserina gansseri LOZ
G.aegyptiaca LOZ
70
75
80
85
90
95
100
105
110
115
120
125
130
135
140
LO Prv. eugubina
LO P. pseudobulloides
HO Prv. eugubina
LO Prv. eugubina
LO C. tenuis
66.04 Ma
LO M.prinsii
LO N.frequens
LO M.murus
HO M.prinsii
LO P.hantkeninoides
HO G.gansseri
LO P.hariaensis
HO G.bulloides
LO R.fructicosa
LO G.linneiana
LO R.powelli
LO P.palpebra
LO G.gansseri
Not included
CC26a
CC25c
NOT STUDIED
Danian
Maastrichtian
CAMP
Paleogene
Cretaceous

Figure 2.9

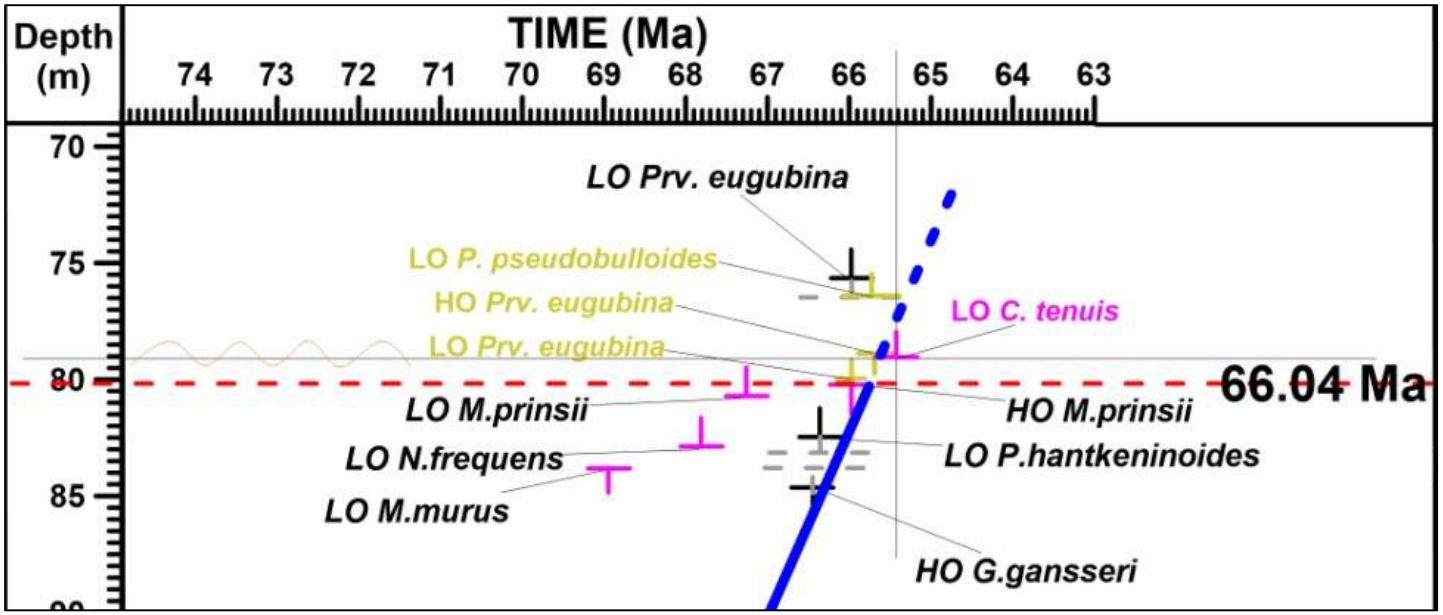
Depth (m)
TIME (Ma)
74
73
72
71
70
69
68
67
66
65
64
63
70
75
80
85
LO Prv. eugubina
LO P. pseudobulloides
HO Prv. eugubina
LO Prv. eugubina
LO C. tenuis
66.04 Ma
LO M.prinsii
HO M.prinsii
LO N.frequens
LO P.hantkeninoides
LO M.murus
HO G.gansseri

Figure 2.10

Table 2.1

Datum Level	**Depth (m)**	**Age (Ma)**
LO *Gansserina gansseri*	137.5	72.99
LO *Pseudoguembelina palpebra*	131.51	71.75
LO *Racemiguembelina powelli*	126.47	71.47
LO *Globotruncana linneiana*	118.12	70.90
LO *Racemiguembelina fructicosa*	110.5	70.14
HO *Globotruncana bulloides*	98.5	68.82
LO *Pseudoguembelina hariaensis*	91.5	67.30
HO *Gansserina gansseri*	84.55	66.49
LO *Micula murus*	83.9	69.00
LO *Nephrolitus frequens*	83	67.84
LO *Plummerita hantkeninoides*	82.5	66.39
LO *Micula prinsii*	80.8	67.30
HO *Micula prinsii*	80.2	66.00
LO *Parvularugoglobigerina eugubina*	75.72	66.00

Table 2.2

Depth (m)	Sample weight (g)	Dry Weight (g)	Split (g)	# of specimens in the split	(*) # of specimens per gram
134.5	13.34	0.3	0.15	260	1733
133.25-.27	11.02	0.32	0.16	704	4400
132.5	11.4	0.36	0.18	644	3578
131.51-.49	6.14	0.18	0.09	578	6422
131-130.98	13.6	0.24	0.12	474	3950
130.47-.51	8.7	0.03	0.015	756	50400
129.47-.50	9g	0.06	0.03	625	20833
128.1	9.7	0.08	0.04	329	8225
127.18-20	8.24	0.06	0.03	377	12567
126.40-.42	10.42	0.24	0.12	754	6283
125.55-.57	9.46	0.1	0.05	679	13580
124.91-.93	10	0.06	0.03	504	16800
124.17-.19	9.12	0.78	0.39	655	1679
123.5	11.13	0.08	0.04	361	9025
122.5	7.54	0.06	0.03	594	19800
121.88-.90	9.2	0.04	0.02	441	22050
121.25	13.64	0.06	0.03	313	10433
120.18-.2	17.65	0.28	0.14	688	4914
119.6	13.54	0.32	0.16	876	5475
118.65-.67	10.92	0.14	0.07	889	12700
118.10-12	12.24	0.2	0.1	988	9880
117.2	9.54	0.14	0.07	777	11100
116.40-.45	11.54	0.26	0.13	956	7353
115.15	15.42	0.2	0.1	361	3610
114.47-50	13.04	0.16	0.08	952	11900
113.19	15.3	0.72	0.36	856	2378
111.91	15.38	0.24	0.12	809	6742
111.4	16.34	0.16	0.08	1421	17763
111.09-10	10.94	0.2	0.1	1055	10550
110.5	20.4	0.54	0.27	770	2852
109.22	14.98	0.44	0.22	564	2564
108.5	12.96	0.26	0.13	720	5538
107.46	15.86	0.8	0.4	1291	3228
106.5	11.92	0.3	0.15	1415	9433
105.89	8.98	0.2	0.1	2165	21650
104.32-.34	7.74	0.24	0.12	801	6675
102.5	11.42	0.1	0.05	524	10480
101.5	8.08	0.52	0.26	1061	4081
100.55-.57	10.36	0.24	0.12	1844	15367
99.8	9.32	0.22	0.11	1798	16345
98.5	12.24	0.16	0.08	1026	12825
97.72	14	0.38	0.19	1398	7358
97.2	16.28	0.34	0.17	684	4024

Depth (m)	Sample weight (g)	Dry Weight (g)	Split (g)	# of specimens in the split	(*) # of specimens per gram
96.5	5.9	0.22	0.11	803	7300
95.5	16.96	0.3	0.15	818	5453
94.25-.22	11.88	0.12	0.06	1475	24583
93.5	12.82	0.06	0.03	276	9200
91.5	20.2	0.3	0.15	1733	11553
90.89-.88	15.26	0.4	0.2	1567	7835
88.70-.68	8.08	0.12	0.06	235	3917
87.47	13.78	0.1	0.05	717	14340
86.45-.42	16.12	1.18	0.59	1080	1831
85.55	10.86	0.2	0.1	527	5270
84.55-.52	8.4	0.28	0.14	1210	8643
83.75-.73	7.46	0.18	0.09	909	10100
82.5	14.3	0.2	0.1	1360	13600
81.05-.02	11.82	0.5	0.25	1329	5316
80.47-.46	**Barren Of Planktonic Foraminifera**				
80.44-.43					
80.4-.39					
80.39-.38					
80.38-.37					
80.34-.32					
79.93-.91					
79.5					
78.5					
77.82					
77.7	19	0.58	0.29	821	2831
76.5	15.68	0.16	0.08	856	10700
75.72-.70	17.66	0.32	0.16	1106	6913
75.6	11.5	0.12	0.06	560	9333
74.45	7.78	0.18	0.09	773	8589

Table 2.2 ends.

Table 2.3.

SR-Lines	Datum Levels (LO/HO)	Thickness (m)	Duration (Myr)	Sedimentation rate (cm/kyr)
SR	LO *Gansserinagansseri* HO *Gansserina gansseri*	52.45	6.48	1.23

Appendix 2.1

Core Depth	PTX%	PSDGMB%	HETEX%	GLBTRN%	RUGO%	Others	SUM	ALL HTX
134.5	7.10	3.79	46.24	4.37	36.33	2.14	100	57.14
133.25	8.16	14.54	61.76	6.37	7.63	1.51	100	84.47
132.5	6.18	2.89	55.00	3.09	30.49	2.33	100	64.07
131.51	10.42	8.42	30.82	1.99	45.45	2.87	100	49.67
131	15.68	29.85	26.49	1.47	19.04	7.44	100	72.03
130.47	11.71	20.71	34.68	5.40	21.17	6.30	100	67.11
129.47	21.10	27.09	29.97	1.43	15.58	4.79	100	78.18
128.1	20.14	34.53	20.14	7.19	7.91	10.07	100	74.82
127.18	20.98	24.69	17.28	22.23	9.87	4.92	100	62.96
126.4	13.38	11.67	17.65	25.66	21.93	9.68	100	42.71
125.55	14.92	16.33	23.66	14.08	25.07	5.91	100	54.92
124.91	17.60	28.52	13.02	12.32	25.00	3.51	100	59.16
124.17	16.54	16.83	15.82	15.10	35.39	0.28	100	49.20
123.5	8.26	30.16	10.33	7.43	40.90	2.89	100	48.76
122.5	10.32	27.52	22.24	7.79	30.73	1.36	100	60.09
121.88	12.97	37.23	17.15	19.24	12.97	0.41	100	67.36
121.25	19.53	43.68	13.80	13.80	8.04	1.13	100	77.01
120.18	12.49	30.87	23.41	8.76	19.94	4.51	100	66.77
119.6	13.35	19.54	28.84	22.24	13.35	2.66	100	61.74
118.65	14.14	16.50	27.44	25.75	13.29	2.85	100	58.09
118.1	14.12	2.28	49.64	18.54	10.41	4.99	100	66.04
117.2	20.89	12.04	28.99	24.57	6.88	6.60	100	61.93
116.4	6.0241	20.36	43.76	14.12	11.11	4.60	100	70.15

Core Depth	PTX%	PSDGMB%	HETEX%	GLBTRN%	RUGO%	Others	SUM	ALL HTX
115.15	24.10	13.39	16.96	22.32	17.85	5.35	100	54.46
114.47	12.43	17.98	33.95	27.05	2.35	6.21	100	64.37
113.19	46.01	8.79	24.18	8.29	7.23	5.48	100	78.99
111.91	51.18	13.90	8.34	10.87	11.56	4.14	100	73.42
111.4	44.9	23.01	14.12	7.48	5.36	5.08	100	82.06
111.09	50.22	14.70	15.15	10.85	2.48	6.56	100	80.09
110.5	42.85	14.51	22.23	15.67	0.23	4.47	100	79.61
109.22	20.60	15.18	41.32	5.85	1.40	15.61	100	77.11
108.5	32.63	13.46	36.06	8.77	1.87	7.18	100	82.17
107.46	48.97	10.26	9.20	12.88	5.80	12.88	100	68.43
106.5	14.58	10.08	47.87	4.71	2.99	19.74	100	72.54
105.89	25.32	6.22	40.81	14.76	5.20	7.67	100	72.35
104.32	27.52	8.70	31.46	21.07	2.79	8.43	100	67.68
102.5	21.61	6.17	45.13	4.27	9.97	12.82	100	72.92
101.5	30.67	8.12	35.00	19.84	3.93	2.41	100	73.80
100.55	34.46	7.17	24.15	4.90	17.48	11.82	100	65.79
99.8	37.34	15.44	26.23	3.59	7.78	9.58	100	79.02
98.5	46.64	5.08	26.75	13.15	5.38	2.97	100	78.48
97.72	36.64	6.61	28.19	10.18	12.02	6.33	100	71.45
97.2	34.11	4.404	25.30	15.93	14.80	5.43	100	63.82
96.5	33.14	3.22	18.82	21.47	17.53	5.79	100	55.18
95.5	19.23	29.80	19.23	8.33	12.82	10.57	100	68.26
94.25	28.15	18.49	25.63	5408678	9.66	13.01	100	72.27
93.5	24.63	10.13	46.38	7641427	8.70	4.35	100	81.15
91.5	29.77	14.33	41.33	1.94	5.60	7.00	100	85.44

Core Depth	PTX%	PSDGMB%	HETEX%	GLBTRN%	RUGO%	Others	SUM	ALL HTX
90.89	27.73	28.29	20.30	8.96	8.40	6.302	100	76.33
88.7	8.26	25.03	43.80	10.38	6.25	6.25	100	77.09
87.47	3.03	21.21	51.51	3.03	9.09	12.12	100	75.75
86.45	25.22	11.23	44.03	6.30	7.68	5.50	100	80.50
85.55	39.47	15.78	35.52	2.63	2.63	3.94	100	90.78
84.55	18.40	14.14	36.64	11.04	13.76	5.99	100	69.19
83.75	43.74	12.51	33.82	4.96	4.96	0	100	90.07
82.5	30.72	9.22	27.36	2.28	19.65	10.74	100	67.31
81.05	45.62	12.65	17.96	2.96	11.71	9.06	100	76.25

Appendix 2.1 ends.

Plate 2.1

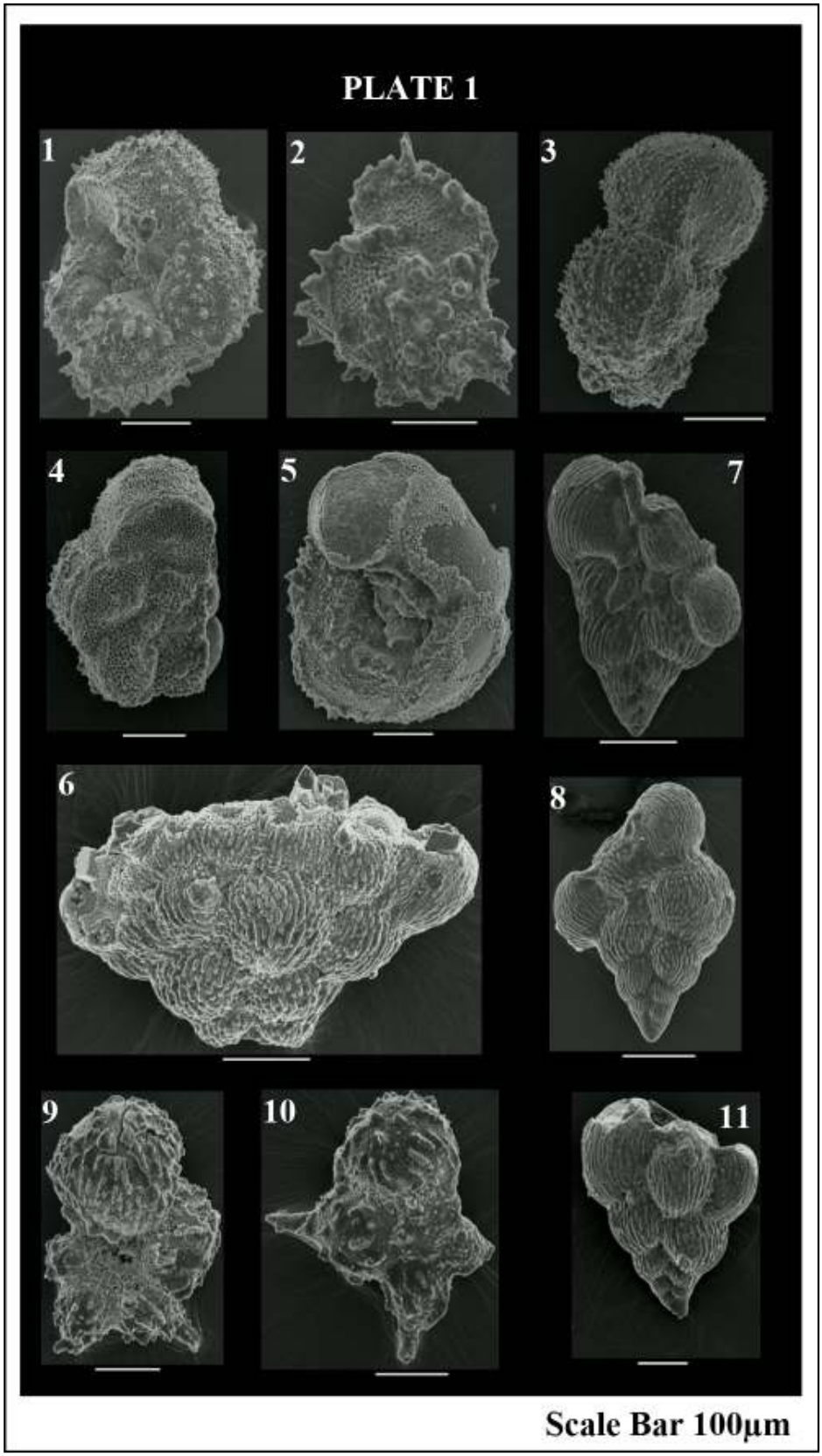

Plate 2.2

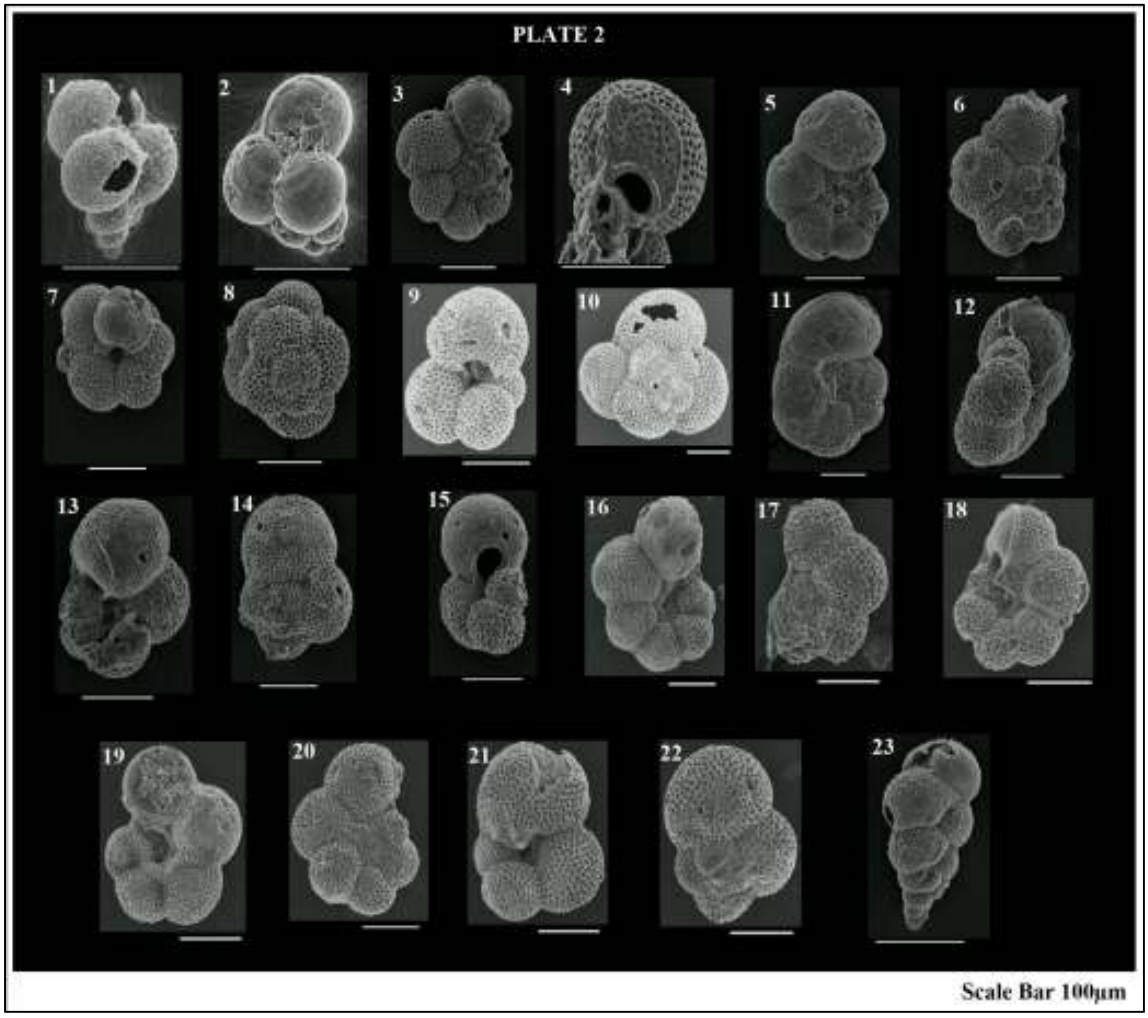
PLATE 2
1
2
3
4
5
6
7
8
9
10
11
12
13
14
15
16
17
18
19
20
21
22
23
Scale Bar 100µm

CHAPTER 3

DATA REPORT

3.1 Introduction

The objectives of this data report are to: 1) determine paleobathymetric estimates and test the reliability of paleodepth estimates using %PF by comparison with paleodepths determined using benthic foraminiferal assemblages; 2) examine the relative abundance (%) patterns between the planktonic foraminiferal assemblages during four intervals in the DQC to develop an understanding for the paleoecological interpretations; and 3) compare the response of the benthic foraminiferal assemblages to that of planktonic foraminifera.

3.2 Material and Methods

3.2.1 Material

The Dababiya Quarry corehole consists of 140 meters of Upper Cretaceous to Lower Eocene mudstones and limestones that are assigned to the Dakhla Shale Formation (DSF), Tarawan Chalk Formation (TCF), and Esna Shale Formation (ESF) (Berggren et al., 2012). The DSF, which is studied here, was tentatively divided into three members and nine units (Dupuis and Knox, 2012; fig. 3.1). Eighty-three samples were taken from Members A, B and the lower part of the C (between 139.87 and 74.45 m). Sixty-six of these samples were taken from Member A, twelve samples were taken from Member B, and the last five samples were taken from the lower part of Member C.

3.2.2 Methods

3.2.2.A Sample Preparation

A new methodology (DAB) based on the use of dilute acidic and basic solutions was developed for this study to extract calcareous microfossils from carbonate and claystone lithologies. The overall preservation of the material was good to excellent.

3.2.2.B Treatment of Data: Planktonic and Benthic foraminiferal assemblages

All benthic and planktonic foraminifera were identified and counted according to procedure described in Chapter 2.

3.2.2.C Treatmeant of Data: P/B Ratio

In addition to the distributions of depth-dependent benthic foraminiferal assemblages, variations in planktonic/benthic foraminifera ratios (P/B ratio) can provide useful insights into paleobathymetric estimates. I determined the error scales on numerical estimates in consideration of the advantages/disadvantages of acidic and basic solutions for disaggregating samples such as etching or dissolution due to overexposure. The question is how sensitive are the paleodepth estimates to the preservational biases induced of the methological procedures (DAB). My results showed that the error on the water depth estimates is greater using equation [1] than equation [2] (fig. 3.4).

The reliability of the numerical methods were tested to estimate water depth variations for Maastrichtian strata in the DQC. This study compared two statistical treatments of the P/B ratio: Equation [1] determined the paleodepth from the PF%-based statistical

approach as proposed by van der Zwaan et al. (1990); and equation [2] determined the paleodepth from the P/B ratio by using the method of Wilson (2003), which was first proposed by de Rijk et al. (1999) (fig. 3.2).

$$D=e^{((\%P+81.9)/24)} \quad \textbf{[1]}$$

$$D=e^{(\%PF*0.03534)+3.58717} \quad \textbf{[2]}$$

where *D* is the estimated paleodepth in meters, *%P* and *%PF* are the percentages of planktonic foraminifera in total numbers of foraminifera in a sample, and *e* is the logarithmic determination of the PF%-based equation.

Equation [3] shows the widely used calculation of PF% values in a sample. In contrast, van der Zwaan et al. (1990) and, more recently, van Hinsbergen et al. (2005) indicated that the exclusion of the stress marker species (S), deep-infaunal benthic species [4]., would yield relatively reliable numeric paleodepth estimates. They implied that the abundance of the *S* species is not controlled by the input of organic matter in the bottom waters, but is ultimately related to riverine input.

$$\%P=\%PF= [P/(P+B)]x100 \quad \textbf{[3]}$$

$$\%P=\%PF= [P/(P+B)-S]x100 \quad \textbf{[4]}$$

In equation [3]: *%P*, and *%PF* are the proportions of planktonic foraminifera in samples, *P* is the number of planktonic foraminiferal specimens; *B* is the number of the benthic foraminiferal specimens.

However, this study did not apply the practice of van der Zwaan et al. (1990) and van Hinsbergen et al. (2005). Berggren and Miller (1989) reported migration events on Cenozoic bathyal and abyssal benthic foraminifera. It is my opinion that none of the benthic foraminiferal assemblages should be excluded from calculations unless a regional and/or a global migration event was not reported. No migration events in Late Cretaceous assemblages in the Mediterranean Tethys sections were reported. Therefore, the traditional P/B ratio calculation given in equation [3] constituted the base of the numeric estimates (fig. 3.3; table 3.1).

3.3 Results

It is widely reported in the literature that *Heterohelix* spp. are markers for low oxygen content in stressful environments (Pardo and Keller, 2008), and *Pseudotextularia* spp. blooms are related with the high nutrient inputs (Olsson et al., 2001). Olsson et al. (2001) reported that *Pseudotextularia elegans* blooms in the central Atlantic sections indicate to the input of nutrient-rich waters from Austral realm. Using these two parameters (oxygen and nutrient) and examining the relative abundance patterns of planktonic foraminifera, I was able to determine the paleoecologic responses of globotruncanids, rugoglobigerinids, and pseudoguembelinids to the changes in environmental conditions during the four stratigraphic intervals in the core. These intervals were determined via considering the *Pseudotextularia* spp., and *Heterohelix* spp. peaks.

The simplistic error estimates as well as the results of both numeric paleobathymetric estimate curves showed that %PF formulas do not provide reliable paleodepth estimates.

These results exhibited ±5 and ±9 meters of change in sea-level based on the absence or presence of one planktonic foraminifera per sample. In addition, the differences in sea-level within subsequent samples unrealistically vary between 200 and 300 meters on a stable shelf. These values also suggest the unreliability of the statistical methods.

Although water depth calculated from the %PF following the formulas [1] and [2] (see above) is rejected in this study (fig. 3.2), the %PF remains indicative of relative change in paleodepth (deeper/shallower) (fig. 3.3). Numerical paleodepths were determined based on the benthic foraminiferal assemblages. In the DQC, benthic foraminiferal assemblages implied that deposition mostly occurred in outer neritic to upper bathyal depths (Midway-Type fauna of Berggren and Aubert, 1975). However, deposition during the latest Maastrichtian (above 97.0 meter) occurred in mid to outer neritic paleodepths (fig. 3.3).

Heterohelix spp. and *Pseudotextularia* spp. are nutrient and oxygen sensitive taxa in surface waters during the Maastrichtian. In the DQC, genera belonging to *Heterohelicidae* family are abundant and diverse. During the four intervals (fig. 3.5; appendix 3.1), the abundances of *Globotruncanidae*, and *Rugoglobigerinidae* never exceeded the abundance of genera belonging to *Heterohelicidae* family. Additionally, *Heterohelix* spp. low abundances are associated with the *Pseudotextularia* spp. high abundances, indicating nutrient enrichment pulses and rapid consumption of nutrients and oxygen in the Upper Nile Valley area. These proxies strengthen the idea of Upper Nile Valley is a part of the North African upwelling belt (Widmark and Speijer, 1997; Soudry et al., 2006; Pardo and Keller, 2008).

Benthic foraminiferal abundances also show stratigraphic patterns (fig. 3.7; appendix 3.2). Some intervals are remarkable with high abundances of some species. These high abundances could also be associated with the changing conditions in the surface water assemblages and can also be used to indicate an upwelling system. However, the last two paleoecologic interpretations require more detailed analysis with higher sampling resolution.

3.4 References

Berggren, W. A. and Aubert, J., 1975. Paleocene benthonic foraminiferal biostratigraphy, paleobiogeography and paleoecology of Atlantic-Tethyan regions: Midway-type fauna. Palaeogeography, Palaeoclimatology, Palaeoecology, 18, 73-192.

Berggren, W.A., and Miller, K.G., 1989. Cenozoic bathyal and abyssal calcareous benthic foraminiferal zonation. Micropaleontology, vol. 35, no. 4, pp. 308-320.

Berggren, W.A., Alegret, L., Aubry, M-P., Cramer, B.S., Dupuis, C., Goolaerts, S., Kent, D.V., King, C., Knox, R.W.O'B., Obaidalla, N., Ortiz, S., Ouda, K.A.K., Abdel-Sabour, A., Salem, R., Senosy, M.M., Soliman, M.F., & Soliman, A., 2012. The Dababiya Corehole, Upper Nile Valley, Egypt: Preliminary results. Austrian Journal of Earth Sciences, vol, 105/1, 161-168.

De Rijk, S., Troelstra, S. R., and Rohling, E. J., 1999. Benthic foraminiferal distribution in the Mediterranean Sea. Journal of Foraminiferal Research, 29: 93-103.

Dupuis, C., and Knox, R.W.O'B., 2012. Lithostratigraphy of the upper Maastrichtian to lower Eocene succession in the Dababiya Corehole, Egypt. Stratigraphy, vol. 9, nos. 3- 4, pp. 205-212.

Olsson, R.K., Wright, J.D., Miller, K.G., 2001. Paleobiogeography of *Pseudotextularia elegans* during the latest Maastrichtian global warming event. Journal of Foraminiferal Research, v. 31, no. 3, p. 275-282.

Pardo, A. and Keller, G., 2008. Biotic effects of environmental catastrophes at the end of the Cretaceous and early Tertiary: *Guembelitria* and *Heterohelix* blooms. Cretaceous Research, 29; 1058-1073.

Soudry, D., Glenn, C.R., Nathan, Y., Segal, I. and VonderHaar, D., 2006. Evolution of Tethyan phosphogenesis along the northern edges of the Arabian-African shield during the Cretaceous-Eocene as deduced from temporal variations of Ca and Nd isotopes and rates of P accumulation. Earth-Science Reviews, 78: 27-57.

Van der Zwaan, G.J., Jorissen, F.J., de Stigter, H.C., 1990. The depth dependancy of planktonic/benthic foraminiferal ratios: Constraints and applications. Marine Geology, 95 (1990) 1-16.

Van Hinsbergen, D.J.J., Kouwenhouven, T.J., Van der Zwaan, G.J., 2005. Paleobathymetry in the backstripping procedure: Correction for oxygenation effects on depth estimates. Palaeogeography, Palaeoclimatology, Palaeoecology, 221 (2005), 245 – 265.

Widmark, J.G.V., and Speijer, R.P., 1997. Benthic foraminiferal assemblages and trophic regimes at the terminal Cretaceous Tethyan seafloor. Palaios 12: 352-369.

Wilson, B., 2003. Foraminifera and paleodepths in a section of the early to middle Miocene Brasso Formation, Central Trinidad. Caribbean Journal of Science, Vol. 39, No. 2, 209 - 214.

3.5 Figure Captions

Figures:

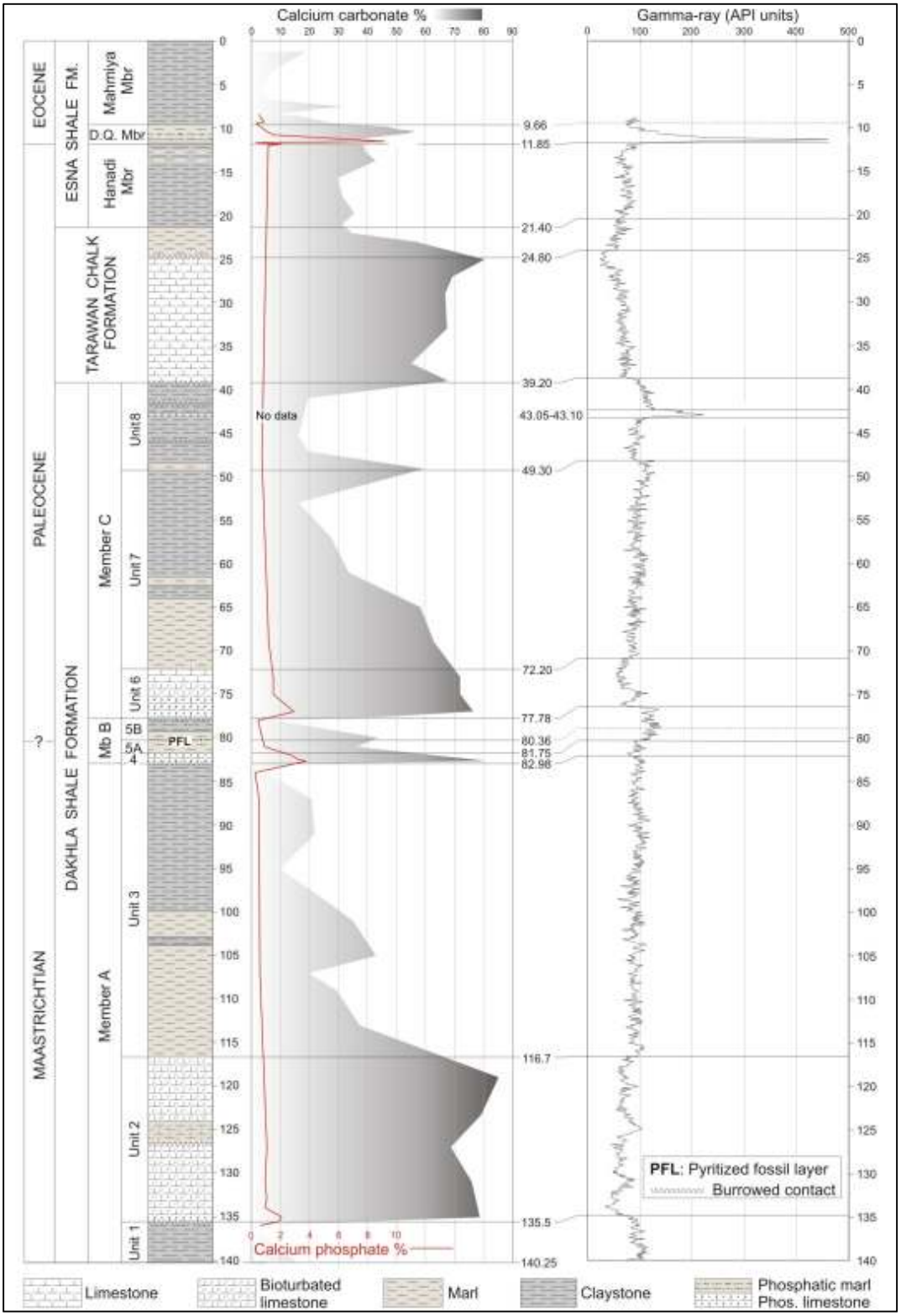

Figure 3.1

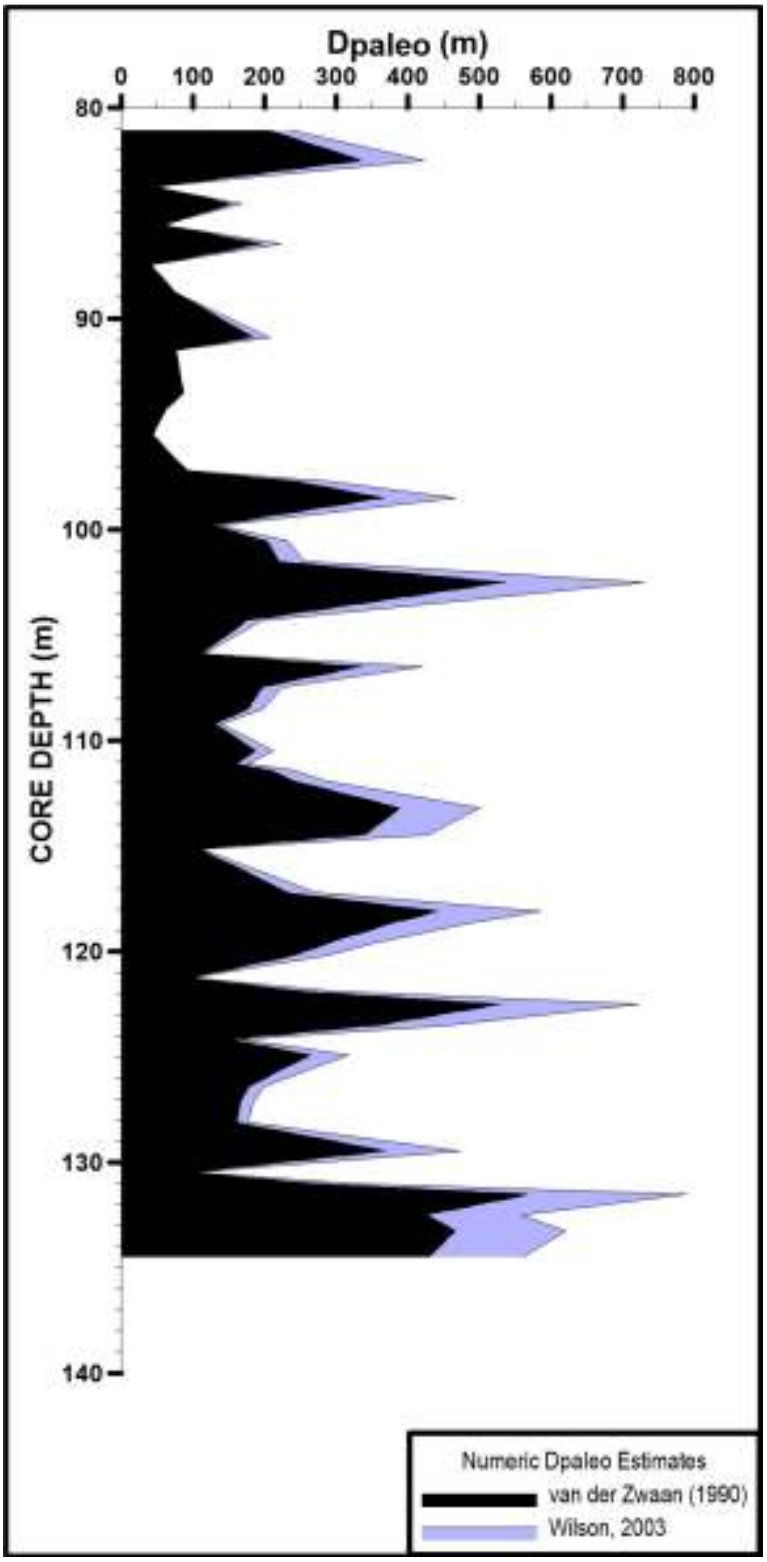
Dpaleo (m)
0
100
200
300
400
500
600
700
800
80
90
100
110
120
130
140
CORE DEPTH (m)
Numeric Dpaleo Estimates
van der Zwaan (1990)
Wilson, 2003

Figure 3.2

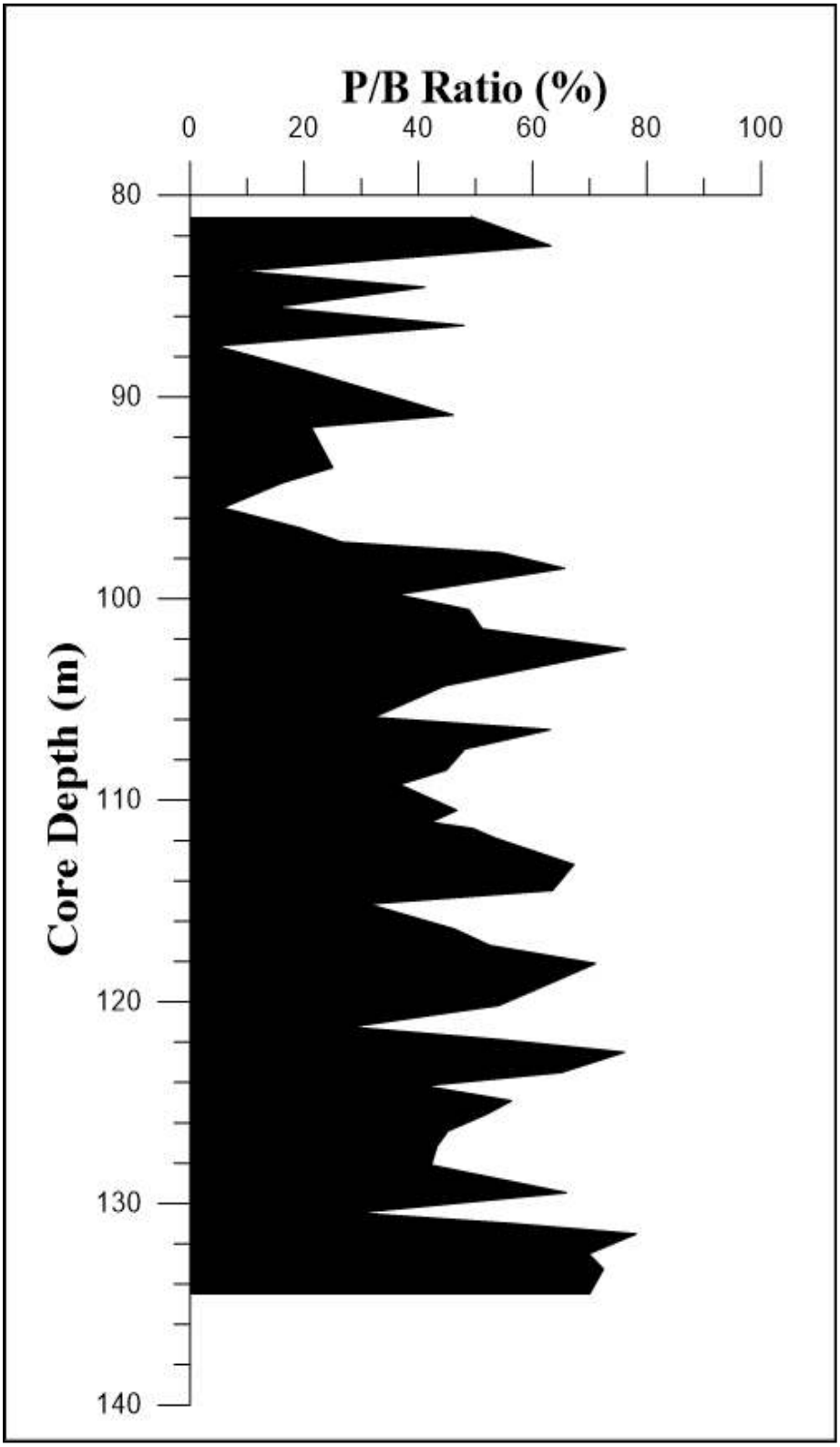

Figure 3.3

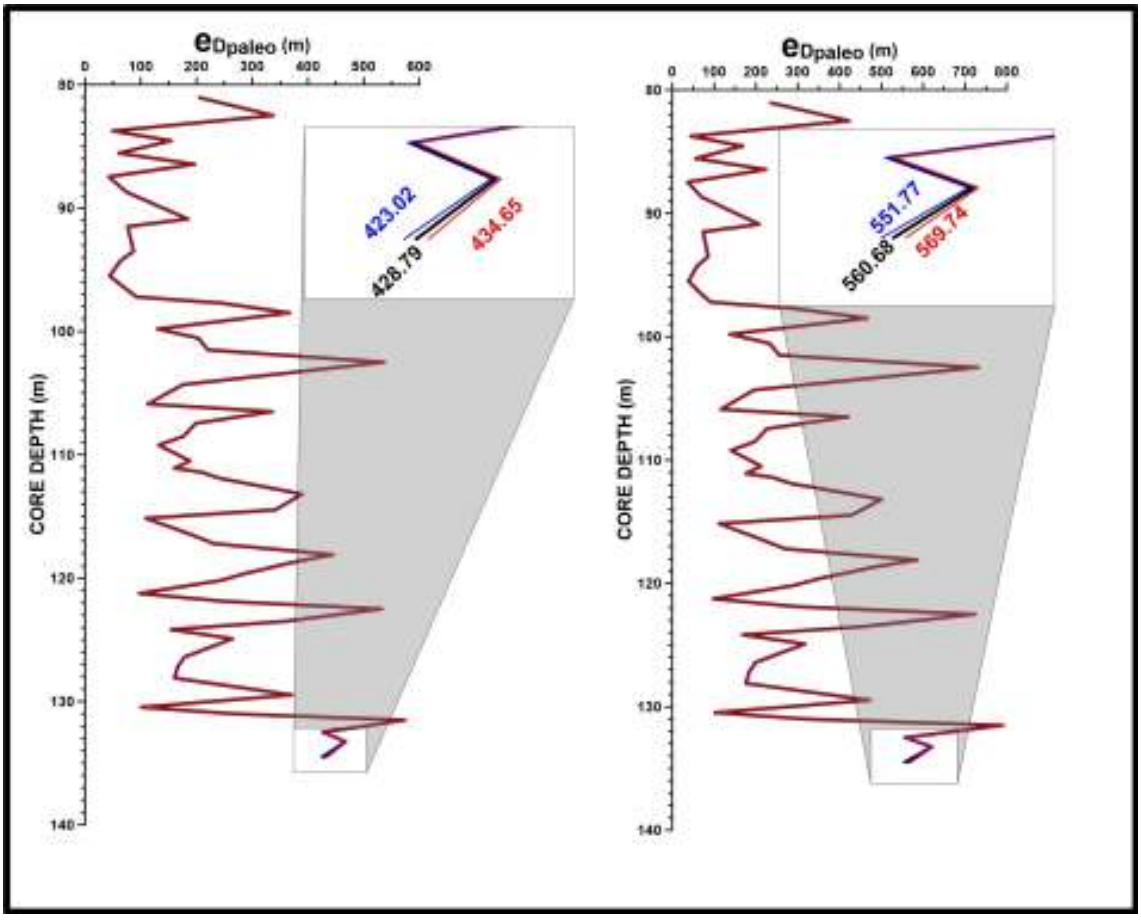
eDpaleo (m)
0
100
200
300
400
500
600
80
90
100
110
120
130
140
CORE DEPTH (m)
423.02
428.79
434.65
eDpaleo (m)
0
100
200
300
400
500
600
700
800
80
90
100
110
120
130
140
CORE DEPTH (m)
551.77
560.68
569.74

Figure 3.4

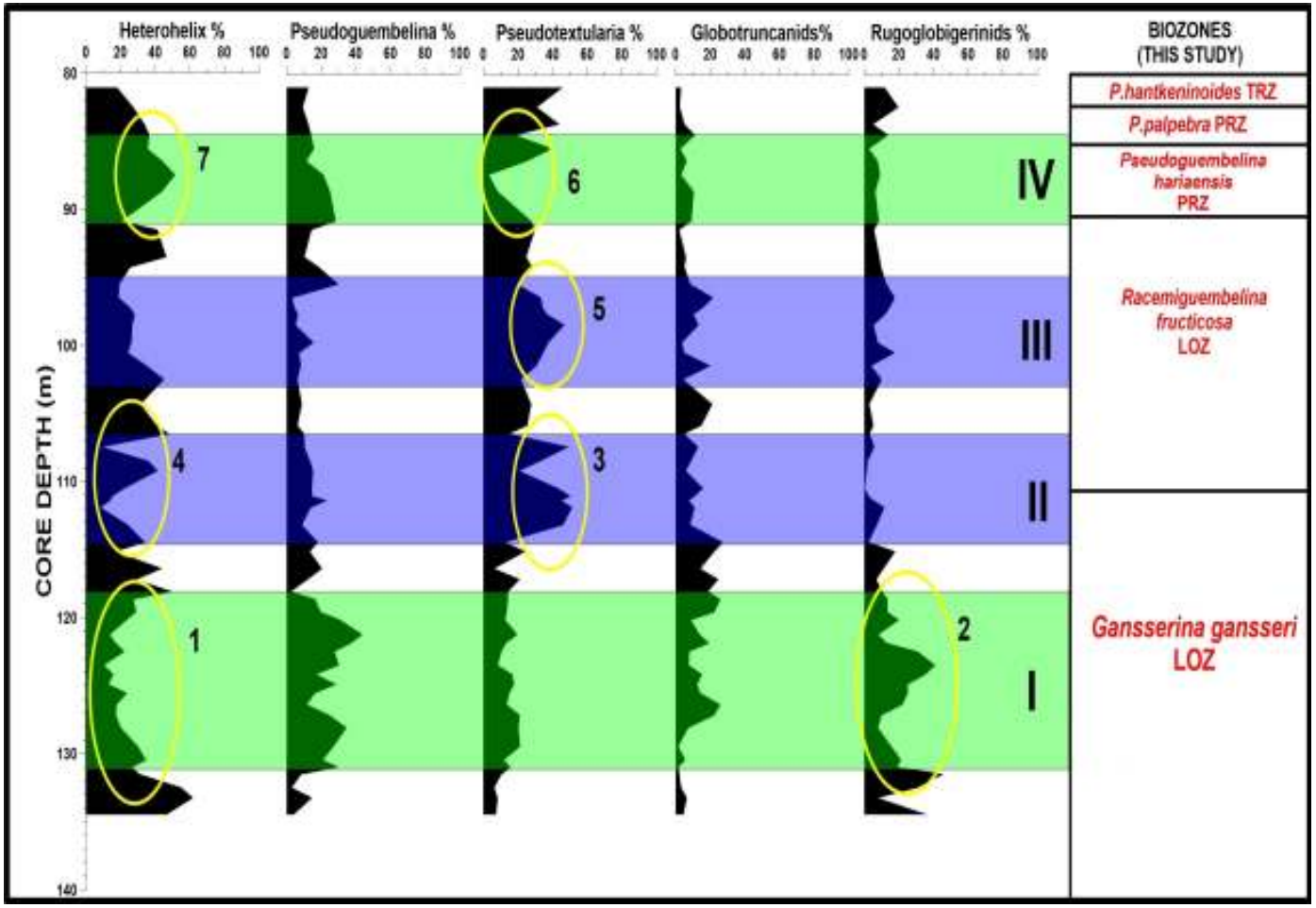
Heterohelix %
Pseudoguembelina %
Pseudotextularia %
Globotruncanids%
Rugoglobigerinids %
0 20 40 60 80 100
CORE DEPTH (m)
80
90
100
110
120
130
140
1
2
3
4
5
6
7
I
II
III
IV
BIOZONES
(THIS STUDY)
P.hantkeninoides TRZ
P.palpebra PRZ
Pseudoguembelina hariaensis PRZ
Racemiguembelina fructicosa LOZ
Gansserina gansseri LOZ

Figure 3.5

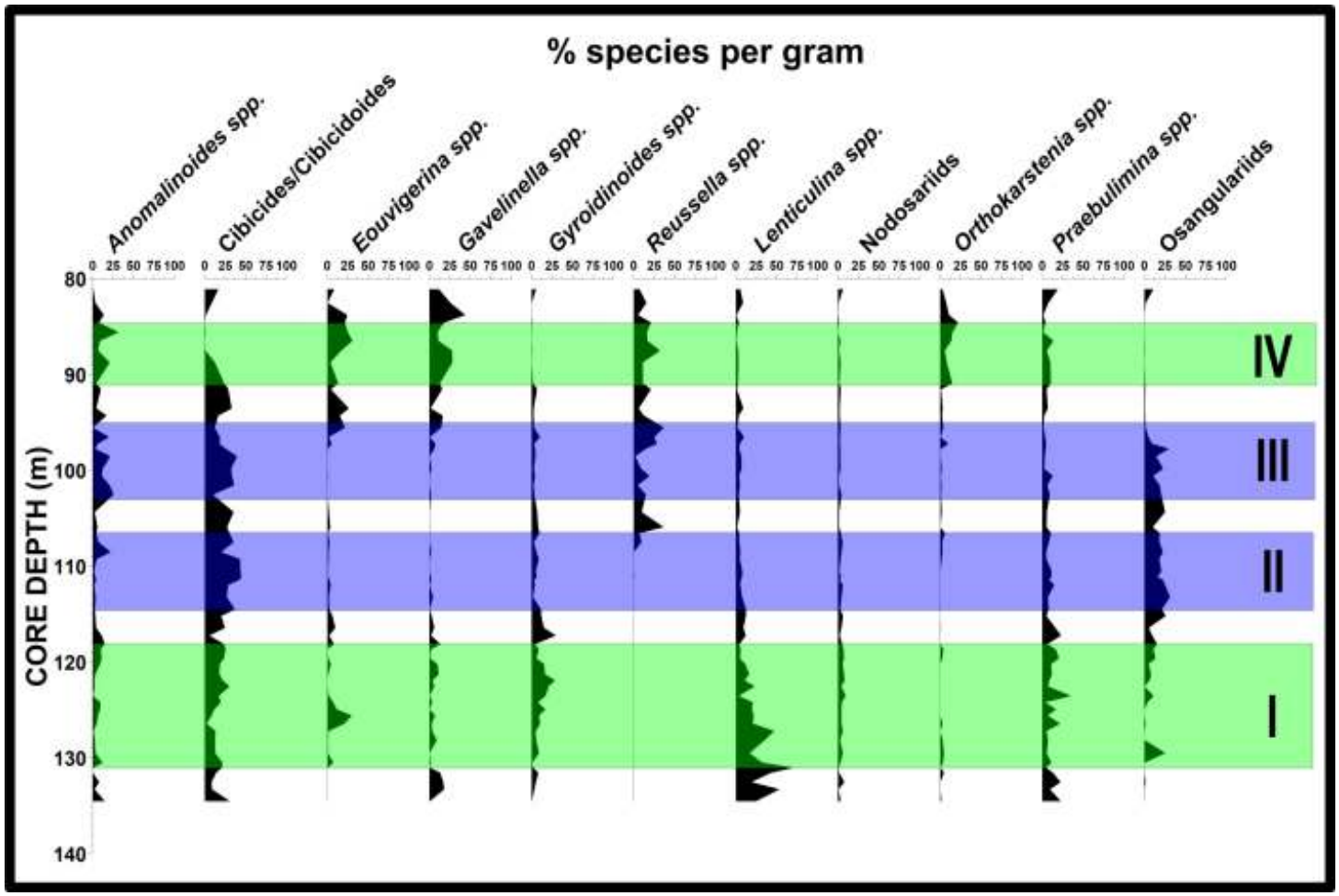
% species per gram
Anomalinoides spp.
Cibicides/Cibicidoides
Eouvigerina spp.
Gavelinella spp.
Gyroidinoides spp.
Reussella spp.
Lenticulina spp.
Nodosariids
Orthokarstenia spp.
Praebulimina spp.
Osangulariids
0 25 50 75 100
CORE DEPTH (m)
80
90
100
110
120
130
140
IV
III
II
I

Figure 3.6

Table 3.1

Core Depth	PF%
134.5	70.00
133.25	72.44
132.5	69.87
131.51	78.20
131	56.54
130.47	29.10
129.47	65.92
128.1	42.24
127.18	43.23
126.4	45.22
125.55	52.13
124.91	56.34
124.17	41.06
123.5	65.09
122.5	76.09
121.88	54.64
121.25	28.11
120.18	54.06
119.6	58.90
118.65	66.59
118.1	71.05
117.2	52.50
116.4	46.44
115.15	31.30
114.47	63.55
113.19	67.28
111.91	53.77
111.4	49.54
111.09	42.18
110.5	46.75
109.22	36.70
108.5	45.00
107.46	48.17
106.5	63.10
105.89	32.19
104.32	44.69
102.5	76.33
101.5	51.17

Core Depth	PF%
100.55	48.91
99.8	36.26
98.5	65.59
97.72	54.36
97.2	26.60
96.5	19.42
95.5	5.74
94.25	16.20
93.5	25.00
91.5	21.23
90.89	46.13
88.7	20.42
87.47	4.60
86.45	47.96
85.55	14.61
84.55	41.15
83.75	8.91
82.5	63.23
81.05	49.20

Table 3.1 ends.

Appendix 3.1

Core Depth	PTX%	PSDGMB%	HETEX%	GLBTRN%	RUGO%	Others	SUM	ALL HTX
134.5	7.10	3.79	46.24	4.37	36.33	2.14	100	57.14
133.25	8.16	14.54	61.76	6.37	7.63	1.51	100	84.47
132.5	6.18	2.89	55.0	3.09	30.49	2.33	100	64.07
131.51	10.42	8.42	30.82	1.99	45.45	2.87	100	49.67
131	15.68	29.85	26.49	1.47	19.04	7.44	100	72.03
130.47	11.71	20.71	34.68	5.40	21.17	6.30	100	67.11
129.47	21.10	27.09	29.97	1.43	15.58	4.79	100	78.18
128.1	20.14	34.53	20.14	7.19	7.91	10.07	100	74.82
127.18	20.98	24.69	17.28	22.23	9.87	4.92	100	62.96
126.4	13.38	11.67	17.65	25.66	21.93	9.68	100	42.71
125.55	14.92	16.33	23.66	14.08	25.07	5.91	100	54.92
124.91	17.60	28.52	13.02	12.32	25.0	3.51	100	59.16
124.17	16.54	16.83	15.82	15.10	35.39	0.28	100	49.20
123.5	8.26	30.16	10.33	7.43	40.90	2.89	100	48.76
122.5	10.32	27.52	22.24	7.79	30.73	1.36	100	60.09
121.88	12.97	37.23	17.15	19.24	12.97	0.41	100	67.36
121.25	19.53	43.68	13.80	13.80	8.04	1.13	100	77.01
120.18	12.49	30.87	23.41	8.76	19.94	4.51	100	66.77
119.6	13.35	19.54	28.84	22.24	13.35	2.66	100	61.74
118.65	14.14	16.50	27.44	25.75	13.29	2.85	100	58.09
118.1	14.12	2.28	49.64	18.54	10.41	4.99	100	66.04
117.2	20.89	12.04	28.99	24.57	6.88	6.60	100	61.93
116.4	6.02	20.36	43.76	14.12	11.11	4.60	100	70.15

Core Depth	PTX%	PSDGMB%	HETEX%	GLBTRN%	RUGO%	Others	SUM	ALL HTX
115.15	24.10	13.39	16.96	22.32	17.85	5.35	100	54.46
114.47	12.43	17.98	33.95	27.05	2.35	6.21	100	64.37
113.19	46.01	8.79	24.18	8.29	7.23	5.48	100	78.99
111.91	51.18	13.90	8.34	10.87	11.56	4.14	100	73.42
111.4	44.92	23.01	14.12	7.48	5.36	5.08	100	82.06
111.09	50.22	14.70	15.15	10.85	2.48	6.56	100	80.09
110.5	42.85	14.51	22.23	15.67	0.23	4.47	100	79.61
109.22	20.60	15.18	41.32	5.85	1.40	15.61	100	77.11
108.5	32.63	13.46	36.06	8.77	1.87	7.18	100	82.17
107.46	48.97	10.26	9.20	12.88	5.80	12.88	100	68.43
106.5	14.58	10.08	47.87	4.71	2.99	19.74	100	72.54
105.89	25.32	6.22	40.81	14.76	5.20	7.67	100	72.35
104.32	27.52	8.70	31.46	21.07	2.79	8.43	100	67.68
102.5	21.61	6.17	45.13	4.27	9.97	12.82	100	72.92
101.5	30.67	8.12	35.00	19.84	3.93	2.41	100	73.80
100.55	34.46	7.17	24.15	4.90	17.48	11.82	100	65.79
99.8	37.34	15.44	26.23	3.59	7.78	9.58	100	79.02
98.5	46.64	5.08	26.75	13.15	5.382	2.97	100	78.48
97.72	36.64	6.61	28.19	10.18	12.02	6.33	100	71.45
97.2	34.11	4.40	25.30	15.93	14.80	5.43	100	63.82
96.5	33.14	3.22	18.82	21.47	17.53	5.79	100	55.18
95.5	19.23	29.80	19.23	8.33	12.82	10.57	100	68.26
94.25	28.15	18.49	25.63	5.04	9.66	13.01	100	72.27
93.5	24.63	10.13	46.38	5.78	8.70	4.35	100	81.15
91.5	29.77	14.33	41.332	1.94	5.60	7.00	100	85.44

Core Depth	PTX%	PSDGMB%	HETEX%	GLBTRN%	RUGO%	Others	SUM	ALL HTX
90.89	27.73	28.29	20.30	8.96	8.40	6.30	100	76.33
88.7	8.26	25.03	43.80	10.38	6.25	6.25	100	77.09
87.47	3.03	21.21	51.51	3.03	9.09	12.12	100	75.75
86.45	25.22	11.23	44.03	6.30	7.68	5.50	100	80.50
85.55	39.47	15.78	35.52	2.63	2.63	3.94	100	90.78
84.55	18.40	14.14	36.64	11.04	13.76	5.99	100	69.19
83.75	43.74	12.51	33.82	4.96	4.96	0	100	90.07
82.5	30.72	9.22	27.36	2.28	19.65	10.74	100	67.31
81.05	45.62	12.65	17.96	2.96	11.71	9.06	100	76.25

Appendix 3.1 ends.

Appendix 3.2

Core Depth	An.	Cib.	Eouvi.	Gavel	Gyroid	Lentic	Nodos	Orthok	Osang	Prbuli	Reuss
134.5	14.59	30.65	0	0	0	24.33	3.16	1.45	0	22.62	0
133.25	2.16	8.67	0	17.86	3.2	53.07	0.52	0	0	9.19	0
132.5	7.58	8.04	0	16.72	5.02	18.73	7.58	0	1.46	22.3	0
131.51	0	13.95	0	12.8	8.07	43.12	1.15	4.61	0	12.8	0
131	0	20.59	0	0	1.71	70.35	0.54	0	0	3.98	0
130.47	11.8	21.47	7.15	1.34	0.67	32.21	2.9	3.35	0	10.96	0
129.47	3.15	12.65	0.62	0	8.85	16.46	5.7	4.42	25.33	5.05	0
128.1	2.35	12.35	0.58	8.82	5.29	35.29	2.35	2.94	0	7.05	0
127.18	0.51	13.02	1.03	3.12	4.68	46.89	5.72	0	0	4.68	0
126.4	4.77	1.96	20.59	2.54	10.43	20.59	3.92	2.81	1.69	21.71	0
125.55	6.32	8.13	29.81	6.62	8.73	21.68	3.91	0	0	6.32	0
124.91	8.72	11.4	11.4	0	16.78	19.46	4.03	0	0	16.78	0
124.17	9.36	19.52	6.96	3.19	7.53	20.43	4.33	0	3.76	3.19	0
123.5	0	16.94	1.694	0	16.94	3.38	9.32	0	11.01	34.74	0
122.5	2.2	30.15	0	5.87	20.59	22.8	3.66	0	0	6.62	0
121.88	1.72	21.83	0	3.44	28.73	10.34	8.04	0	6.32	8.62	0
121.25	3.03	17.68	1	11.11	16.16	16.16	7.06	0	8.08	11.61	0
120.18	8.75	18.25	4.16	9.5	15.21	11.42	5.33	0	4.91	10.67	0
119.6	10.6	23.02	1.02	0.68	5.67	4.93	7.09	2.43	13.44	20.19	0
118.65	9.58	25.29	0	1.53	8.8	5.74	6.49	3.81	10.74	16.48	0
118.1	14.4	23.45	7.81	13.16	3.7	4.11	4.93	0	15.22	5.76	0
117.2	10.9	5.45	2.16	1.8	29.48	12	1.8	0	9.45	22.93	0
116.4	3.92	24.53	9.57	5.61	14.96	9.06	3.92	0.47	5.13	15.95	0
115.15	3.01	19.82	6.03	2.58	11.63	12.06	6.03	0	25.86	4.74	0

Core Depth	An.	Cib.	Eouvi.	Gavel	Gyroid	Lentic	Nodos	Orthok	Osang	Prbuli	Reuss
114.47	2.45	36.83	2.13	0	11.34	12.27	2.45	0	21.16	7.662	0
113.19	3.38	26.69	1.49	4.06	1.49	7.45	4.06	0	31.16	6.77	0
111.91	1.52	28.41	4	0	4	5.22	5.56	0	25.03	14.5	0
111.4	4.13	42	2.23	2.06	2.91	5.85	1.72	0	22.72	8.26	0
111.09	2.88	44.4	0.72	1.26	6.31	7.4	3.42	0	15.7	10.64	0.72
110.5	1.53	43.37	0.42	0	4.72	7.66	1.53	0	20.6	11.34	0.18
109.22	4.5	42.91	1.28	0	8.72	4.5	2.86	1.57	17.88	4.86	0
108.5	21.95	19.56	1.17	1.8	5.71	5.4	4.18	2.7	22.54	4.5	0
107.46	6.85	35.1	2.35	0	2.68	4.03	5.37	2.35	18.15	7.86	9.41
106.5	4.21	29.97	0.41	0	9.5	3.8	3.16	5.7	18.37	10.55	6.74
105.89	5.66	26.91	3.5	0.25	7.91	1.25	1.25	0	10.08	5	36.33
104.32	2.19	35.15	1.69	0	6.59	4.86	1.2	1.69	25.13	5.36	9.52
102.5	25.4	9.83	0	1.63	3.27	3.27	4.09	0.81	20.49	9.01	14.75
101.5	20.38	35.96	0	0	2.19	4.84	1.09	1.32	18.41	5.94	4.84
100.55	11	33	0.64	0	4.18	3.78	1.037	0.51	10.46	12.57	19.11
99.8	11.9	32	0	2.22	2.62	6.66	2.82	1.61	22.71	2.42	8.88
98.5	21.15	39.45	0	0	4.45	6.51	2.44	0.39	14.22	2.83	1.62
97.72	2.85	25.51	0.48	5.71	4.2	3.88	2.5	0.48	29.91	3.88	14.52
97.2	5.82	17.92	5.11	7.21	3.01	4.63	2.06	9.79	9.31	4.63	28.19
96.5	19.6	18.33	1.63	0	9.88	9.7	2.19	0.36	4.76	3.28	24.93
95.5	0	12.04	21.35	14.47	2.86	2	2.86	3.87	1.41	1.57	36.69
94.25	16.75	16.4	15.09	15.97	2.09	3.22	1.83	2.09	0.95	2.17	12.21
93.5	4.16	32.76	26.2	1.17	2.37	8.93	1.78	2.96	0.58	6.54	5.95
91.5	9.7	28.55	4.03	15.37	6.53	1.15	3.07	0.95	1.05	4.9	20.95
90.89	4.34	23.6	13.16	12.61	1.76	2.44	1.49	14.78	1.08	10.31	11.12

Core Depth	An.	Cib.	Eouvi.	Gavel	Gyroid	Lentic	Nodos	Orthok	Osang	Prbuli	Reuss
88.7	20.61	12.13	3.64	27.9	0	3.02	3.02	7.86	0	9.69	10.92
87.47	6.41	0.73	16.84	27.47	0.54	2.74	1.09	5.67	0.54	5.31	32.05
86.45	8.68	0	30.55	10.82	0.11	0.67	2.81	13.52	0.33	13.52	16.57
85.55	31.26	0.99	24.81	9.67	0.24	1.24	0	14.88	0	0.99	15.88
84.55	7.23	0	21.26	17.57	0.6	3.54	1.38	21.89	0	3.84	21.11
83.75	13.43	1.22	24.18	43.6	0	0.48	0.24	10.62	0	0.96	5
82.5	3.05	8.47	0	25.64	0	8.7	0.47	7.29	1.41	7.29	15.52
81.05	0.47	16.4	8.35	11.19	5.36	5.2	5.99	2.68	10.88	19.08	6.78

Appendix 3.2 ends.